MAGNETIC BASED CELL SORTING IN MICROFLUIDIC DEVICES

A Thesis Submitted to
the Graduate School of Engineering and Sciences of
İzmir Institute of Technology
in Partial Fulfillment of the Requirements for the Degree of

MASTER OF SCIENCE

in Bioengineering

by
Hatice Ahsen ÖZCAN

July 2024
İZMİR

We approve the thesis of **Hatice Ahsen ÖZCAN**

Examining Committee Members:

Assoc. Prof. Dr. Hüseyin Cumhur TEKİN
Department of Bioengineering, İzmir Institute of Technology

Prof. Dr. Engin ÖZÇİVİCİ
Department of Bioengineering, İzmir Institute of Technology

Assoc. Prof. Dr. Sinan GÜVEN
Department of Medical Biology, Dokuz Eylül University

16 July 2024

Assoc. Prof. Dr. Hüseyin Cumhur TEKİN
Supervisor, Department of Bioengineering,
İzmir Institute of Technology

Assoc. Prof. Dr. Ceyda ÖKSEL KARAKUŞ
Head of the Department of
Bioengineering

Prof. Dr. Mehtap EANES
Dean of the Graduate School of
Engineering and Science

ACKNOWLEDGEMENTS

First and foremost, I express my sincere gratitude to my supervisor Assoc. Dr. H. Cumhur TEKİN for his continuous support, invaluable advice, and guidance throughout the entire research and writing process of this thesis.

I extend my sincere thanks to the members of my thesis progress and dissertation committee, Prof. Dr. Engin ÖZÇİVİCİ, and Assoc. Dr. Sinan GÜVEN for dedicating their valuable suggestions, comments, and time to this thesis.

I am deeply grateful to thank the members of the Biomedical Micro and Nano Systems Laboratory (LBMS) for all their efforts and for creating a highly productive laboratory environment. I also thank the faculty members of the Bioengineering Department at IZTECH, for sharing their knowledge and experience with me during this Master's program.

I acknowledge the financial support from The Scientific and Technological Research Council of Turkey for the 2210-C BIDEB Domestic Priority Areas Master's Scholarship Program and the Izmir Institute of Technology Research Fund (grant number: 2023IYTE-1-0047).

Apart from all the thanks, I would like to express my endless love and gratitude to my mother, Sevdiye Sönmez Özcan, my father, Fatih Özcan, my brother, Abdullah Beren Özcan, my sister, Elif Meva Özcan, and my friends. Your infinite support and unwavering encouragement have been the cornerstone of my journey. Your love, kindness, and belief in me have been a constant source of strength and inspiration. Thank you for being there through every high and low point in my life and for always standing by my side no matter what. Last but not least, I would like to thank myself for putting in all the hard work.

ABSTRACT

MAGNETIC BASED CELL SORTING IN MICROFLUIDIC DEVICES

Blood can serve as a diagnostic and therapeutic tool by isolating disease-associated cells, or biomarkers, from complex samples. Among these biomarkers, circulating endothelial cells (CECs) are vital for identifying cardiovascular diseases and cancer. Their precise separation is challenging, leading to the development of a label-free microfluidic system. This system leverages Magnetic Levitation principles to separate CECs from white blood cells (WBCs) using magnetic, gravitational, and drag forces. The microfluidic chip has one inlet and two outlets: the top outlet collects low-density Human Umbilical Vein Endothelial Cells (HUVECs) as a mimic of CECs, while the bottom outlet collects high-density U937 cells as a mimic of WBCs using a withdrawal method. To optimize sorting efficiency, various concentrations of gadolinium (Gd^{3+}) and different flow rates and ratios were tested. Adjusting flow rate ratios between the outlets created a virtual separator, enhancing sorting efficiency. Using 30 mM Gd^{3+} at a withdrawal rate of 0.2 mL/h achieved an 86.67 ± 10.4% sorting efficiency for HUVECs and 20.83 ± 7.93% for U937 cells. Additionally, using the same microfluidic chip, live/dead MDA-MB-231 cancer cell separation was performed. The purpose of live/dead sorting was to obtain live cells for use in tissue engineering applications, specifically spheroid formation, as higher numbers of live cells increase spheroid formation efficiency. Using 75 mM Gd^{3+} with a total flow rate of 0.25 mL/h achieved a sorting efficiency of live cells at 77.87 ± 9.82% and dead cells at 11.02 ± 5.81% from the top outlet.

ÖZET

MİKROAKIŞKAN CİHAZLARDA MANYETİK TABANLI HÜCRE AYRIŞTIRMASI

Kan, hastalıkla ilişkili hücreleri heterojen örneklerden ayırarak hastalık teşhisi ve tedavisi için kullanılır. Bu hücrelerin bazıları, örneğin damar hasarı ve kanser için biyobelirteçler olarak kullanılan dolaşımdaki endotel hücreleri (CEC'ler) gibi nadirdir. Bu nadir hücrelerin kesin olarak ayrılması çok önemli ve zordur. Bu sorunu çözmek için etiketsiz bir mikroakışkan sistem geliştirildi. Bu sistem, parçacıkları etiketlemeden belirli konumlara kaldırmak için manyetik, yerçekimsel ve sürükleme kuvvetlerinden yararlanan Manyetik Levitasyon ilkelerini kullanarak CEC'leri beyaz kan hücrelerinden (WBC'ler) izole eder. Mikroakışkan çipin bir girişi ve iki çıkışı vardır: üst çıkış, CEC'lerin bir taklidi olarak düşük yoğunluklu İnsan Göbek Ven Endotel Hücrelerini (HUVEC'ler) toplarken, alt çıkış, bir geri çekme yöntemi kullanarak WBC'lerin bir taklidi olarak yüksek yoğunluklu U937 hücrelerini toplar. Ayrıştırma verimliliğini optimize etmek için paramanyetik ortam olarak kullanılan gadolinyumunun (Gd^{3+}) çeşitli konsantrasyonları, akış hızları ve oranları test edildi. Çıkışlar arasındaki akış hızı oranlarının ayarlanması, sanal bir ayraç oluşturarak ayıklama verimliliğini artırdı. Toplam 0,2 mL/saat geri çekme akış hızıyla 30 mM Gd^{3+} kullanılması, üst çıkıştan HUVEC'lerin %86,67 ± 10,4'te ve U937 hücrelerinin %20,83 ± 7,93'te ayrıştırma verimliliğine ulaştı. Ek olarak, aynı mikroakışkan çip kullanılarak canlı/ölü MDA-MB-231 kanser hücresi ayrımı gerçekleştirildi. Canlı/ölü ayırmanın amacı, daha fazla sayıda canlı hücrenin sferoid oluşum verimliliğini arttırması nedeniyle, sferoid oluşum gibi doku mühendisliği uygulamalarında kullanılmak üzere canlı hücreler elde etmekti. Toplam 0,25 mL/saat geri çekme akış hızıyla 75 mM Gd^{3+} kullanılması, üst çıkıştan canlı hücrelerin %86,03 ± 2,54'te ve ölü hücrelerin %11,02 ± 5,81 oranında ayrıştırma verimliliğine ulaştı.

TABLE OF CONTENTS

LIST OF FIGURES

Figure **Page**

Figure **Page**

LIST OF ABBREVIATIONS

RBCs	red blood cells
WBCs	white blood cells
CTCs	circulating tumor cells
CECs	circulating endothelial cells
FACS	fluorescence-activated cell sorting
MACS	magnetic-activated cell sorting
MAGLEV	magnetic levitation
HUVECs	human umbilical vein endothelial cells
PDMS	polidimetilsiloxane
HCl	hydrochloric acid

CHAPTER 1

INTRODUCTION

The blood contains a diverse range of cells that serve as fundamental components of the human body.[1] Two main types of components are circulating cells and biomolecules. The circulating cells include Red Blood Cells (RBCs) (3.5-5.9 x 10^{12} cells/L), White Blood Cells (lymphocytes, monocytes, and granulocytes) (WBCs) (4.5-11.0 x 10^{9} cells/L), and platelets (150-400 x 10^{9} cells/L).[2] The biomolecules consist of lipids, proteins, and nucleic acids. The exact numbers of these components depend on factors such as age and gender.[3] In clinical settings, blood is primarily used as a body fluid for diagnostic purposes. To utilize blood for these purposes, disease markers must be sorted out. Therefore, cell sorting, and enrichment methods are crucial tools for disease diagnosis and treatment.[4] Cell sorting is a method used to separate disease-associated cells from complex or heterogeneous samples. These sorted cells typically serve as biomarkers, providing crucial information that facilitates precise decisions for disease management.[5] Among these cells, some of them are rare cells that present less than 1000 cells per mL, such as circulating endothelial cells (CECs) and circulating tumor cells (CTCs) which occur at frequencies of approximately 1 per 10^{6} nucleated cells in the blood.[6,7] Precise separation and identification of these rare cells are crucial for diagnostic and pharmacological purposes.[8]

CECs, are mature endothelial cells, that exhibit elevated counts in response to various conditions including vascular damage (such as acute myocardial infarction, hypertension, and coronary artery disease), sickle cell anemia, cancer, and post-organ transplantation.[9–11] Consequently, they hold promise as indicators for prognosis and treatment response assessment.

In the literature, various methods have been explored for cell separation or sorting, which can broadly be categorized into physical force-based techniques (including filtration, micro/nanostructured surfaces, and density gradient centrifugation depending on physical properties such as size, stiffness, deformability, density, and electric charges)

and affinity-based techniques (such as immunoaffinity, which necessitates a labeling process).

1.1. Conventional Cell Sorting Methods

General standard methods for cell sorting include antibody binding-based flow cytometry, which relies on fluorescence-stained and magnetic-activated cells.

1.1.1. Fluorescence-Activated Cell Sorting

Fluorescence-Activated Cell Sorting (FACS) is applied to sort and then analyze targeted cells from a heterogeneous mixture depending on their fluorescent properties, it is a flow cytometry technique.[12] Developed by Bonner in 1972 to isolate mouse spleen cells[13], FACS involves labeling target cells with fluorescent probes on their surfaces before they flow through the machine. The system first detects the fluorescent markers and then monitors changes in the intensity of emitted light as cells pass through, directing them into appropriate tubes using electrostatic forces (Figure 1.1).[14] Different types of lasers can be used in FACS depending on the specific tests being conducted, with common wavelengths nm including 488 and 603, as well as 375, 405, 445, and 561.[15] This technique allows for both quantitative and qualitative analyses. While all cells emit and absorb light, cells labeled with fluorescent molecules exhibit altered emission signals. FACS is not time-consuming once standardized, but it requires a large sample volume, typically around 1 mL.[16] Additionally, labeling steps must be performed without cross-contamination to ensure an efficient sorting rate.

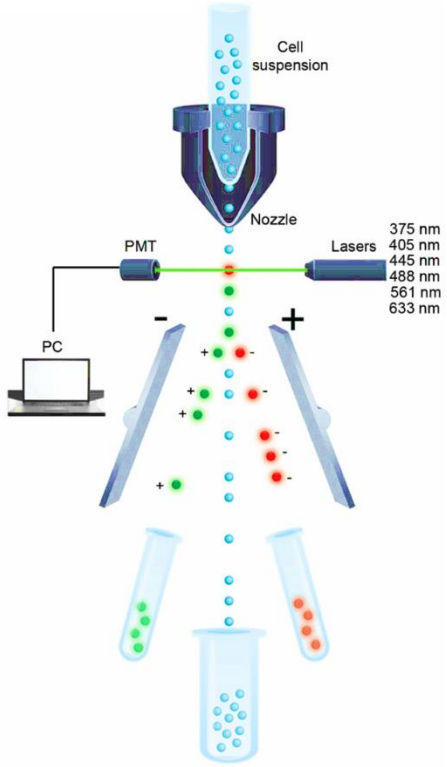

Figure 1.1. Illustration of Fluorescence Activated Cell Sorting (FACS) Technique.[15]

1.1.2. Magnetic-Activated Cell Sorting

Magnetic-Activated Cell Sorting (MACS) is another immunolabeling procedure likely to FACS. In MACS, instead of fluorescent labeling, magnetic beads are implemented to label the target cells' surfaces before the separation steps.[17] Once the cells are labeled, the cell mixture is passed through an externally created magnetic field. The targeted cells are retained by the magnetic field, while non-targeted ones pass through and are discarded.[18] Afterward, the external magnetic field is shut down, and elution steps are performed to collect the labeled cells (Figure 1.2). MACS is a comparatively simple and cost-effective system. However, the labeling must be homogeneous, and the experiment duration should be minimized to prevent cell loss.[16]

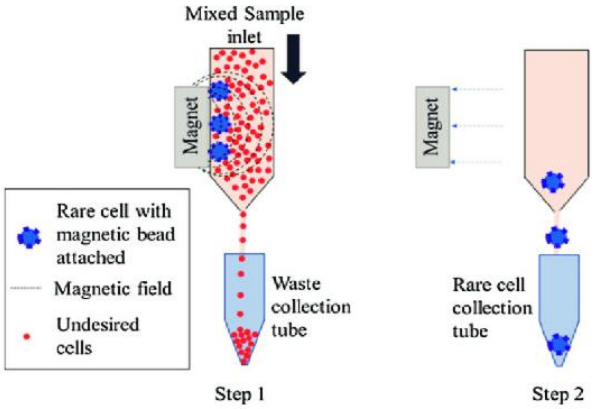

Figure 1.2. Illustration of Magnetic Activated Cell Sorting (MACS) Technique.[19]

These two separation techniques, FACS, and MACS, are widely used as cutting-edge instruments in clinical settings. While each method has its own advantages, their drawbacks have encouraged the advancement of cell sorting systems depending on microfluidics. These systems offer a powerful and different approach, providing cost-effective, highly efficient isolation, with a high purity, and subsequent analysis of different cell types.[20]

1.2. Microfluidic Based Cell Sorting

Microfluidics has attracted significant research interest because of its many benefits including the need for low sample volumes and enabling easy and controllable fluid manipulations and particles like microparticles and cells.[21] Additionally, microfluidics demonstrates excellent mimicry of physiological conditions.[22] By eliminating scientist-dependent steps and implementing automation, the risk of contamination decreases significantly. Moreover, the integration of various technologies and the ability for parallel processing reduce both the processing time and cost.[23] Given their precise manipulation abilities, microfluidics finds wide application in the separation of microparticles, particularly cells. Cell separation involves isolating or selecting target cells from a background or heterogeneous mixture for use in diagnostics and drug

development.[24] Cell sorting, or cell separation in microfluidics, can be based on both physiological (label-free) and biochemical (labeled) characteristics of the cell. Physiological properties may include size, density, shape, elasticity, surface proteins, and deformability.[25] Biochemical properties encompass magnetic, electrical, fluorescence, and immunologic properties.[22] Cell sorting methods can also be classified as either active or passive categories based on whether an external force is used.[25]

1.2.1. Affinity-Based Cell Separation

Cell sorting based on chemical attributes involves affinity-based separations, which require labeling steps. In microfluidics, both the chip surfaces and the cell surfaces are typically treated with affinity ligands.[26] Cells without labels pass through the microfluidic chip, while labeled cells are captured by the chip surfaces. After the capturing step, non-target cells are discarded, and the targeted cells are eluted using various methods and collected for further analysis.[27] A crucial aspect of this sorting technique is the selection of appropriate ligands.

1.2.2. Cell Separation Based on Physical Properties

Cell sorting depends on physical attributes in microfluidic devices that utilize size, density, shape, and deformation potential to distinguish target cells from heterogeneous mixtures.[28] This label-free method eliminates the need for expensive labeling processes, thereby reducing sample preparation time and increasing cell viability.

1.2.2.1. Size Based Cell Separation

Separation based on size can be achieved using porous filters that isolate rare cells while allowing target cells to pass through and retaining non-target cells, or using physical barriers like micropillar structures which capture the targeted cells and let others flow through.[29]

1.2.2.2. Density and Magnetic Susceptibility Based Cell Separation

Magnetic-based cell separation, or magnetophoresis, requires an external magnetic field. Positive and negative magnetophoresis are the main categories of magnetophoresis.[30] In positive magnetophoresis, targeted cells are magnetically labeled, as seen in techniques like MACS. Conversely, negative magnetophoresis does not require labeling. Instead, it leverages the difference in magnetic susceptibility between target cells (which are typically diamagnetic) and the surrounding medium (usually a paramagnetic salt solution or ferrofluids) to achieve separation.[31] An external magnetic field is necessary for magnetic manipulation.

Contact-free and power-free cell separation or enrichment methods leverage differences in magnetic susceptibility and density, aided by gravitational force.[32] Magnetic Levitation (MagLev) is a novel technique utilizing negative magnetophoresis (Figure 1.3). Cells are put into a paramagnetic medium in this method and placed under a nonuniform magnetic field. After some time, the cells levitate where magnetic and buoyancy forces balance each other. Each cell type has a specific density, allowing MagLev to separate cells based on even small differences in density.[33]

To implement this, two magnets are placed that have the same poles facing each magnetother, and a capillary channel is positioned between them. Since cells generally do not have magnetic susceptibility, a paramagnetic medium, such as Gadolinium (Gd^{3+}), is required to demonstrate the effect of the magnetic field. In this medium, diamagnetic cells have a tendency to levitate in a direction of a point where the magnetic force (F_M) and the buoyant force (F_B) are equal. This magnetic force is proportional to the density

differences between the cell and the medium, which is a unique property for all cell types. With MagLev, even small density differences between two different cells can be exploited for effective separation.[7] In general, F_M the magnetic force can be applied to a magnetic particle of volume, V, χ_c and χ_m represent the magnetic susceptibilities of the cells and the paramagnetic medium, respectively, μ_0 is the permeability of free space is expressed as Equation (1.1):

$$F_M = \frac{V(\chi_c - \chi_m)}{\mu_0} (\vec{B}.\nabla)\vec{B} \quad , \; F_B = V(\rho_c - \rho_m)g \tag{1.1}$$

, where $\vec{B}$ a magnetic induction, F_B, the buoyant force can be applied to a magnetic particle of volume, V, with a difference of ρ_m and ρ_c are the densities of the medium and the cells, respectively. g is the gravity.

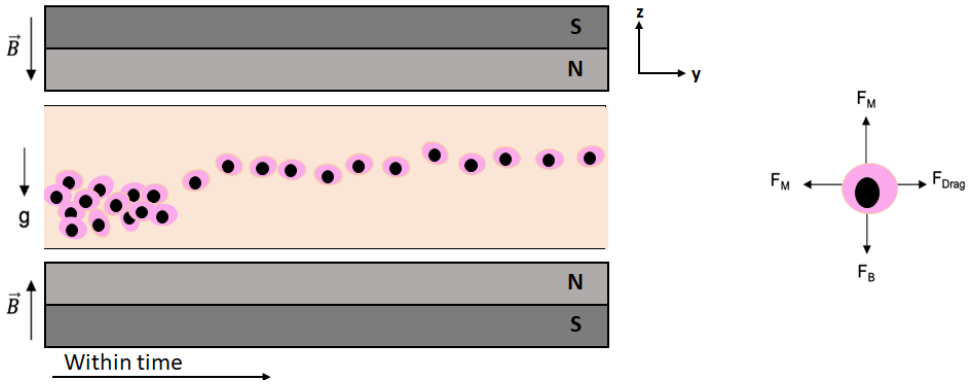

Figure 1.3. Schematic of Magnetic Levitation (MagLev) principle.

MagLev has numerous biomedical applications, including measuring the density of microparticles and cells, observing and measuring protein[34], and antigen-antibody binding[35], and sorting rare and targeted cells for diagnostic methods such as cancer[6] and sickle cell[36] disease detection. Additionally, MagLev is used in 3D cell culturing and tissue engineering.[37,38] This technology can be integrated with smartphones, imaging

systems[39], image processing, and artificial intelligence[40], to enhance its versatility and portability in resource-limited settings.

1.3. Aim of the Thesis

The aim of this study is to obtain a cost-effective, and reusable MagLev platform for separating endothelial cells from blood cells without any need for complicated, expensive, and bulky devices that require specially trained personnel. The platform and microfluidic system are designed to operate without cell labeling, enhancing cost efficiency. This system can be used repeatedly for different applications.

Endothelial cells are not generally found circulating in the blood and are present in low numbers. However, their number increases in persons with cardiovascular diseases. Although there is an increase in their number, their quantity concerning the other circulating cells remains low, making their separation challenging. The technology can be used to diagnose cardiovascular disease by sorting CECs from whole blood. Additionally, the isolated CECs can be used for further analyses in personalized medicine and treatment methods.

This same separation technique has been used for sorting live cancer cells from dead cancer cells, an important step in tissue engineering applications to initiate 3D cell culturing with a high number of viable cells. This separation technique enables the effective separation of live cells from dead ones. The live cells can then be used for spheroid formation using hanging drop technology. The results show that spheroid formation can occur both stably and efficiently when a high number of live cells are used in the hanging drop method.

CHAPTER 2

MAGNETIC LEVITATION-BASED ENDOTHELIAL CELL SORTING

This chapter explains the importance of sorting CECs and the development of a MagLev-based microfluidic sorting system. It starts with an overview of the state of CEC research. Then, the design of the platform and the experimental procedures are given. Finally, the results of the sorting experiments using the MagLev platform are discussed. To simulate endothelial cells, Human Umbilical Vein Endothelial Cells (HUVECs), and to mimic white blood cells, the U937 cell line is used.

2.1. State of the Art Circulating Endothelial Cell Sorting in Microfluidic Devices

Endothelial cells are important in the exchange of metabolites between tissues and blood and line the inner surfaces of all circulatory structures.[41] CECs are mature cells that shed from the vascular lining and start to circulate due to mechanical, chemical, or pathological conditions, such as cardiovascular diseases, immune disorders, and certain cancers like breast cancer.[16] An increase in their number indicates that something is amiss. Clinically, the number of CECs should be approximately one in a million nucleated cells.[42] Therefore, an elevated number of CECs can serve as a biomarker for the diagnosis of diseases and treatment purposes. In clinics, their detection has been done using FACS and MACS.[9]

In the literature, various methods exist for sorting CECs in microfluidic systems, including magnetic bead labeling and size-based separation. A microfluidic disk was developed for immunomagnetic-based CEC separation.[43] The microfluidic disk consists

of three main components: an inlet, connecting channels, and waste reservoirs. The mixture of immunomagnetically labeled (targeted) and non-targeted cells is placed into the inlet reservoir. The labeled CECs are trapped at the inlet by a multistage magnet positioned directly above it. As the chip rotates, the other cells flow through the connecting channels into the waste reservoirs. Subsequently, the chip is observed using a fluorescence microscope. Target cells are detected, and their numbers are observed on the disk using the microscope.

A novel microfluidic device for detecting magnetic bead-labeled cells was developed.[44] This device features two identical counter mechanisms within the fluid chamber, where an externally created magnetic field is applied (Figure 2.1). Targeted cells, labeled with antibody-functionalized magnetic beads, experience a decrease in velocity due to magnetic interactions as they flow through the chamber, whereas non-targeted cells continue to flow unimpeded into the second chamber. The device identifies targeted cells based on their transit time delay.

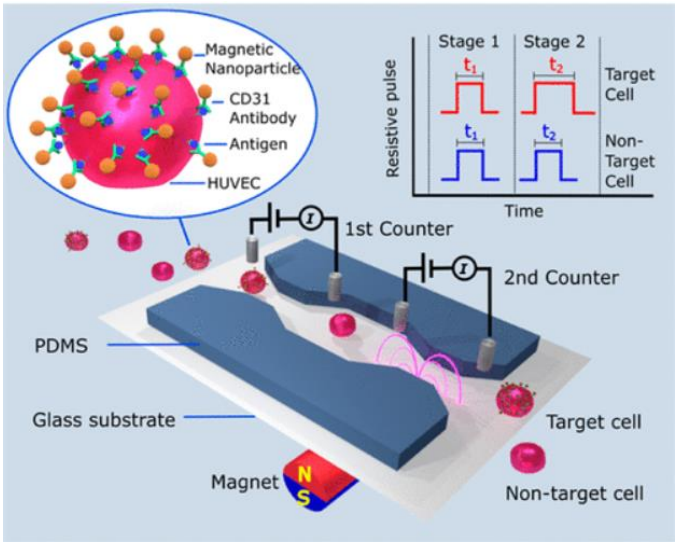

Figure 2.1. Schematic of the magnetic-functionalized HUVEC Cell Assay. HUVECs pass through an externally created magnetic field. The targeted cells pass from the first micro-Coulter counter to the second one with delayed transit time and lower speed, while non-targeted cells maintain the same transit time.[44]

A microfluidic chip with spatially staggered micropillars was improved to capture CECs.[45] The micropillars consist of three elliptic-cylindrical capture units: two of them for the side walls and one for capturing, designed to retain CECs in the capturing area (Figure 2.2). After the capturing procedure, all cells were fixed to the capture units and stained with immunofluorescence staining. Following the washing steps, the chip was read out using a fluorescence microscope for the identification and enumeration of CECs. The capture efficiency varied with flow rate: 87.8 ± 3.7% at 0.5 mL/h, 82.8 ± 2.9% at 1 mL/h, 71.4 ± 4.2% at 1.5 mL/h, and 64.6 ± 4.0% at 2 mL/h, with a concentration of 100 HUVECs/mL. However, this system has drawbacks. Not all cells fall within the same diameter range, which can reduce sorting efficiency. Additionally, clogging by larger cells can prevent target cells from capturing.

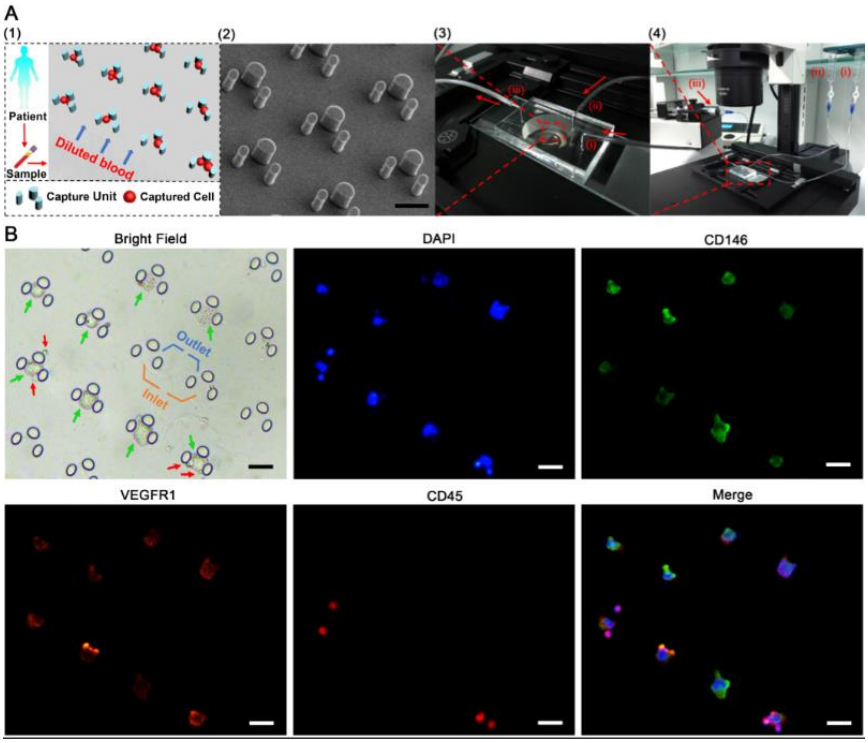

Figure 2.2. Isolation of CECs in microfluidic systems. (A) The design of a microfluidic system for isolation of CECs. (1) Illustrative diagram, the working principle of the microfluidic chip when blood enters the system. (2) SEM image showing the microcapillary and capture units in detail. (3) Microfluidic chip image. (4) Required instruments. (B) Immunofluorescent labeling of isolated HUVECs. Scale Bar indicates 50 μm.[45]

An innovative strategy for multiplex rare cell enumeration of CECs was implemented using an automated filtration system.[46] The device features a filter membrane with 8 μm pores, allowing non-target cells like WBCs to pass through while retaining the CECs on the filter. The target cells are fluorescently stained before filtration. After filtration, the targeted cells are stabilized on the chip and observed under a fluorescence microscope.

This thesis presents a novel technique for CEC separation from blood cells. The sorting system was designed in a manner that did not need the use of complicated, bulky, and expensive devices, and labeling steps. Utilizing magnetic levitation principles, this cost-effective platform allows for the diagnosis of cardiovascular diseases by sorting CECs from blood cells. Additionally, separated CECs obtained through this technology can be used for sensitive analyses in personalized medicine, transplantation monitoring, and regenerative medicine. Consequently, the technology developed in this thesis will have a variety of applications in medicine, enhancing diagnostic precision and treatment strategies.

2.2. Materials and Methods

2.2.1. Fabrication of Polydimethylsiloxane (PDMS) Microfluidic Chip

The previous design of the Chromium (Cr) Mask was used for the manufacturing of the Polydimethylsiloxane (PDMS) microfluidic chip.[6] The microfluidic chip which used in the sorting experiments contains one inlet, one separator, and two outlets (Figure 2.3).

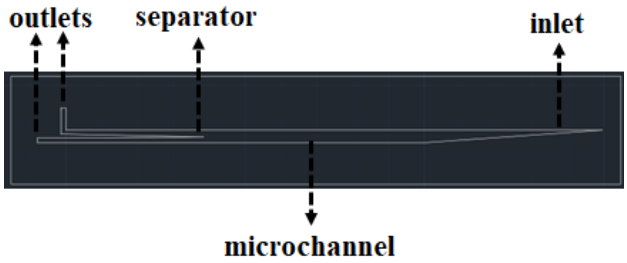

Figure 2.3. The designed microfluidic chip. It consists of one inlet, a separator in the middle of the channel, and two outlets.

PDMS is a commonly used polymer for microfluidic device manufacturing due to its various advantages, such as optical transparency (allowing microparticles to be observed under a microscope), nontoxicity, and biocompatibility.[47] The PDMS was prepared using two components: a silicone elastomer base and a curing agent, the mixture of 10:1 ratio, respectively.[48] The mixture was well stirred until transparent and then the removal of bubbles was placed in a desiccator. Once bubble-free, the mixture was poured onto a silicon wafer covered by 3D-printed molds and left in an oven at 65°C overnight (Figure 2.4). After the curing, the replica PDMS with the microchannel was taken off, and inlets and outlets were created using punches. Since PDMS is hydrophobic and does not easily bond with surfaces without treatment, both the glass and PDMS surfaces underwent air plasma treatment to enable covalent bonding.[49] After the treatment of air plasma, the PDMS was bonded to the surface of the glass, making the PDMS microfluidic chip ready for use (Figure 2.4).

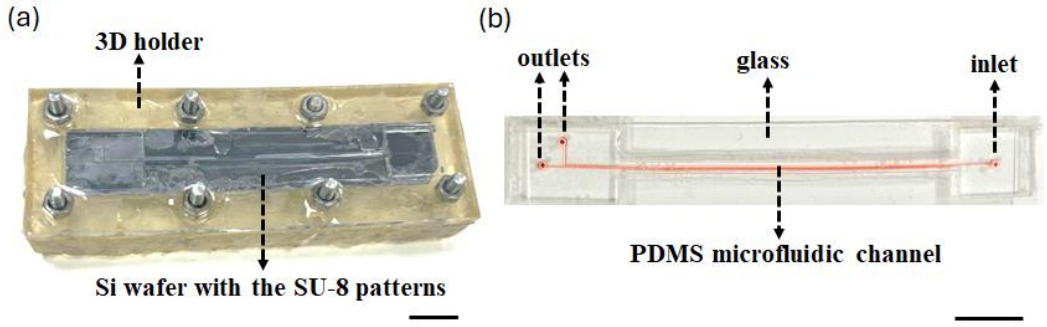

Figure 2.4. The fabrication of PDMS Microfluidic Channel. (a) The mold used for the manufacturing of the PDMS microfluidic chip. (b) The ready-to-use PDMS microfluidic chip. Scale Bars indicate 1 cm.

2.2.2. Development of the Magnetic Levitation (MagLev) Platform for Capillary and Polydimethylsiloxane (PDMS) Microfluidic Chip Observation

The MagLev platform for capillary and PDMS Microfluidic Chip observation is required to observe the cell with an inverted microscope. To do so the design was done. In order to observe the cell the 45-degree tilted mirrors were used, and the mirror's distance was calculated with respect to the working distance of the microscope. The platform contains two N52-grade neodymium magnets the dimensions of the magnet are a length of 50 mm, a width of 2 mm, and a height of 5 mm. These magnets are placed on the same poles face each other. In between the magnets, there was a hole for capillary which was designed as the capillary measurements a length of 50 mm in length, a width of 1 mm, and a height of 1 mm. The 3D body of the platform was printed out using Formlabs, Form3 3D printer with clear resin, and the magnets and mirrors were assembled to the body (Figure 2.5).

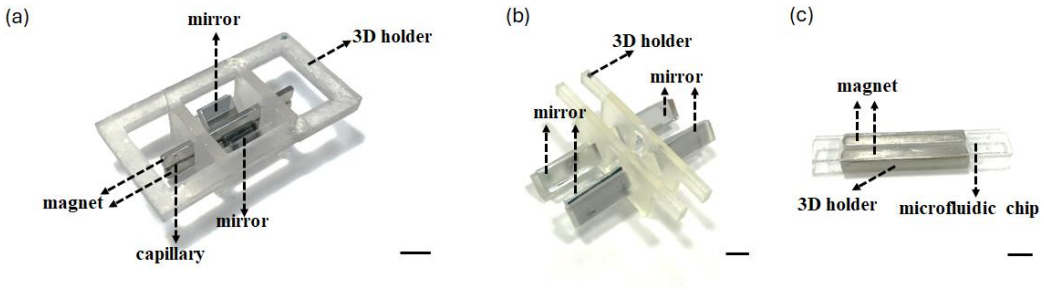

Figure 2.5. The developed magnetic levitation platforms. (a) The magnetic levitation platform for the capillary channel consisting of two 45° tilted mirrors, two magnets, a hole for a capillary channel, and a 3D-printed holder. (b) The magnetic levitation platform for the PDMS microfluidic chip consisting of 45° tilted mirrors, a 3D-printed holder, and a hole for the PDMS microfluidic chip. (c) The PDMS microfluidic chip holder consisting of two magnets, a hole for a PDMS microfluidic channel, and a 3D-printed holder. Scale Bars indicate 1 cm.

2.2.3. Cell Culture

U937 human monocyte cells were cultured in Roswell Park Memorial Institute 1640 (RPMI 1640, Euroclone) medium containing 10% fetal bovine serum (FBS, ECS0180, Euroclone) and 1% Penicillin-Streptomycin (Penicillin/Streptomycin 100×, Euroclone). Human Umbilical Vein Endothelial Cells (HUVECs) were cultured in Dulbecco's Modified Eagle Medium high glucose (DMEM, Gibco) supplemented with 10% FBS and 1% Penicillin-Streptomycin. [50] The cells were placed in an incubator set to 37°C with 5% CO_2. When the cells reached the desired growth stage, they were used in experiments.

The preparation of cells for experiments was done in two ways due to their adhesiveness. HUVEC cells exhibit adhesive properties, while U937 cells are suspended. U937 cells were centrifuged for 5 minutes at 1200 rpm, the supernatant was discarded, and the remaining cells were resuspended in 1 mL of RPMI. The desired cell concentration was then used for the experiments.

For HUVEC cells, the supernatant was discarded from the flask, and Trypsin (Trypsin-EDTA, Euroclone) was added to detach the cells. Cell detachment was carried out at 37°C for 10 minutes, followed by centrifugation for 5 minutes at 1200 rpm. The remaining cells were resuspended in 1 mL of DMEM, and the desired cell concentration was used for the experiments.

2.3. Results and Discussion

2.3.1. Magnetic Levitation of HUVEC and U937 Cells in Capillary

For MagLev experiments in capillaries, U937 and HUVEC cells were used at a concentration of 10^3 cells/mL. A paramagnetic solution of Gadavist (Gd^{3+}, Bayer) was added to the cells at molarities ranging from 10 mM to 50 mM and 100 mM. Prepared solutions of 30 µL were loaded into capillary channels. Following 15 minutes, the images were captured at 5× magnification using an inverted microscope (Zeiss Axio Vert A1, Germany) (Figure 2.6).

The levitation height of cells in the MagLev platform was assessed using the ImageJ program. The distance from the bottom magnet to the center of each cell was measured. Average levitation heights were calculated for all concentrations and cell types, and t-tests were conducted (Figure 2.7). In both HUVECs and U937 cells the average levitation heights were identified to be significantly different across all Gd^{3+} concentrations. Additionally, an increase in the Gd^{3+} concentration resulted in a higher levitation height. These results show that the optimal Gd^{3+} concentration may vary depending on the application. Using a low Gd^{3+} concentration is important to achieve the maximum difference in average levitation height of the two cells. For instance, at a concentration of 10 mM, the difference in average levitation height between HUVECs and U937 cells was 65 µm, while it was 32 µm at 50 mM. These findings suggest that optimizing Gd^{3+} concentration can enhance endothelial cell sorting using the principle of MagLev.

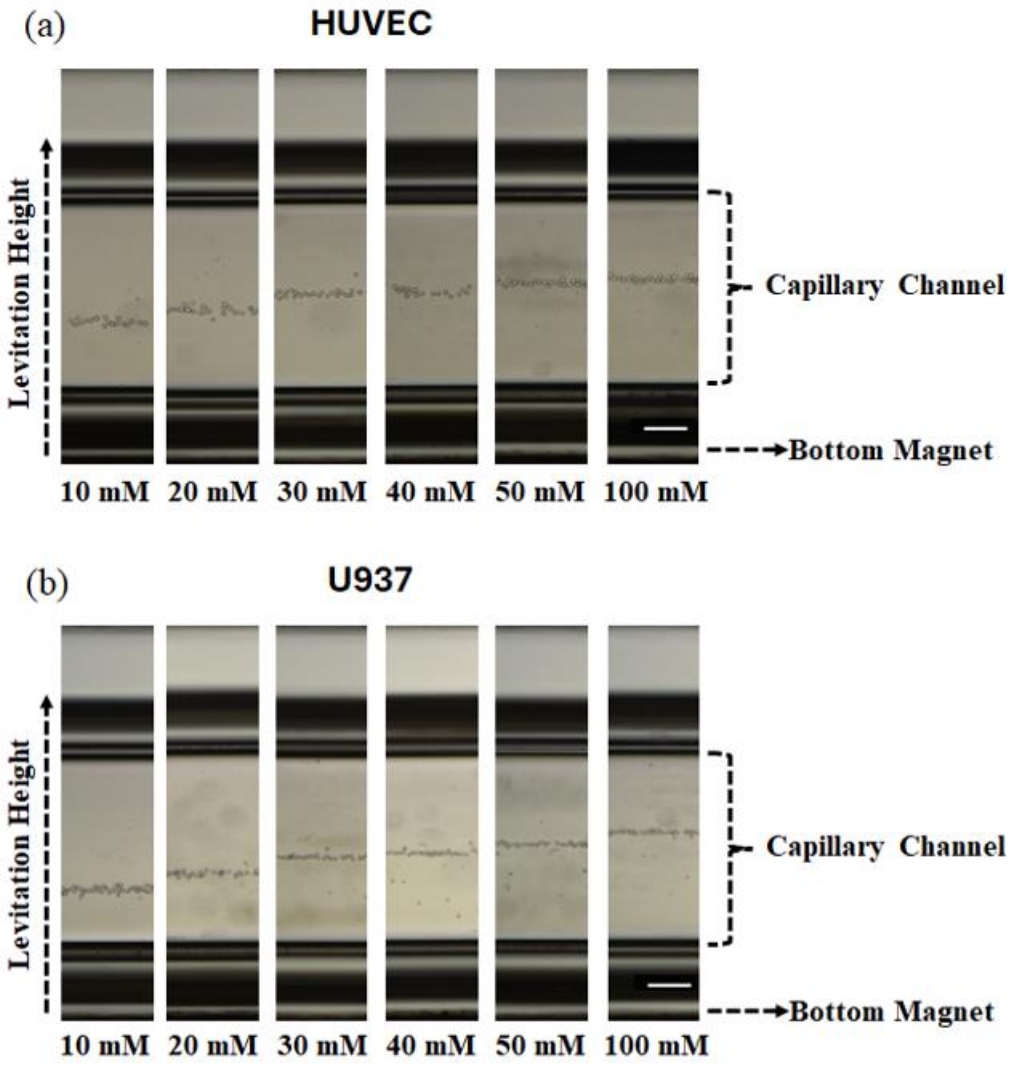

Figure 2.6. The micrographs of levitated cells with varying Gd^{3+} concentrations (10 to 50, and 100 mM). (a) HUVECs and (b) U937 cells were used in the experiments. Scale Bar indicates 200 μm.

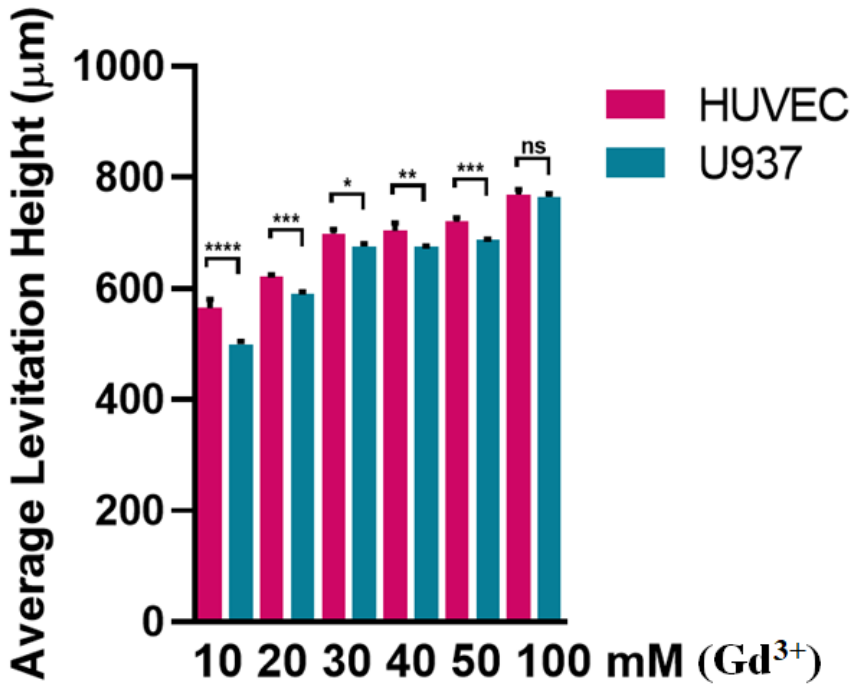

Figure 2.7. The graph of average levitation heights of HUVECs and U937 Cells.

2.3.2. Magnetic Levitation-based HUVEC and U937 Cells Static Condition in PDMS Microfluidic Chip

For sorting experiments under static conditions in the PDMS microfluidic chip, U937 and HUVEC cells were used at a concentration of 10^4 cells/mL. These cells were analyzed under static conditions separately to determine the optimum average levitation height difference. After cell calculation, a paramagnetic medium with different concentrations (10 - 50 mM) was added to the solution. Prepared solutions of 20 µL were loaded into the microfluidic chip. Following 15 minutes, the images were captured at 10× magnification using an inverted microscope (Zeiss Axio Vert A1, Germany) (Figure 2.8). The levitation height of cells in the MagLev platform was assessed using the ImageJ program. The distance from the bottom magnet to the center of each cell was measured. Average levitation heights were calculated for all concentrations and cell types, and t-tests were conducted (Figure 2.9).

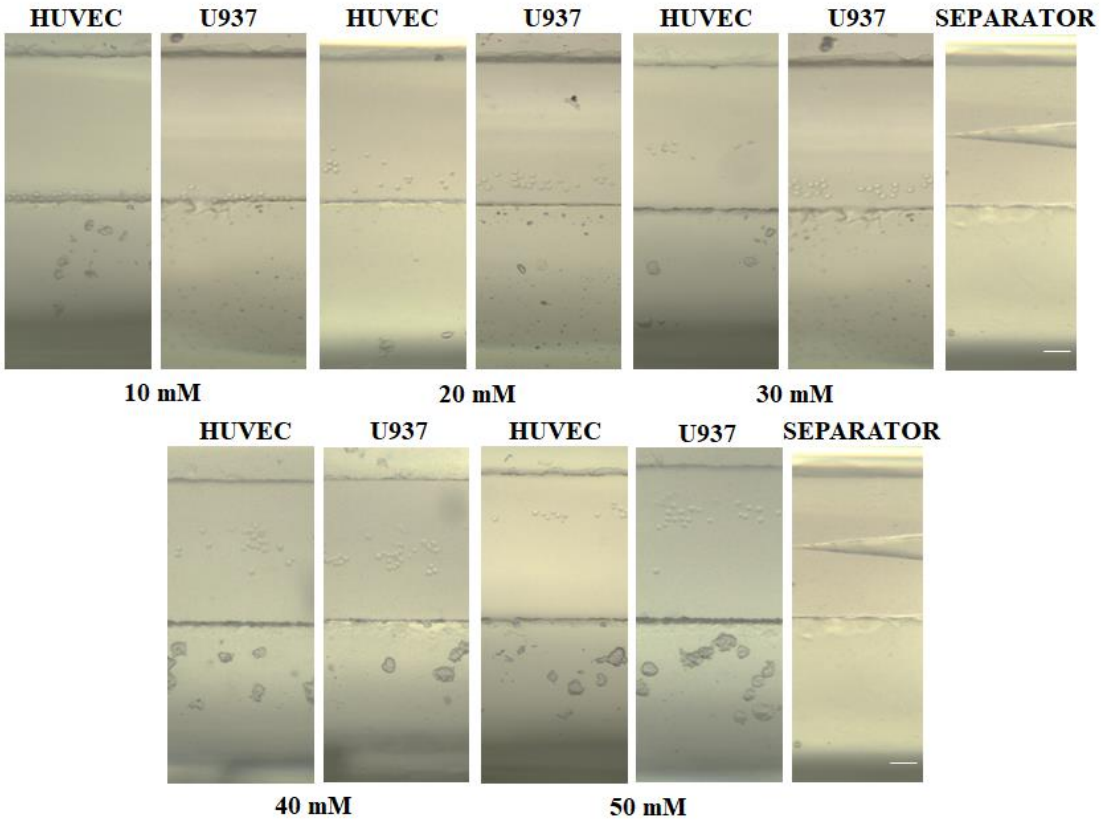

Figure 2.8. The micrographs of levitated cells with varying Gd^{3+} concentrations (10 to 50 mM) HUVECs and U937 cells. Scale Bar indicates 100 μm.

In the experiments, HUVECs did not concentrate above the separator due to their lower density compared to U937 cells, which settled at the bottom. The closest approximation to the desired separation was achieved with a 30 mM Gd^{3+} concentration.

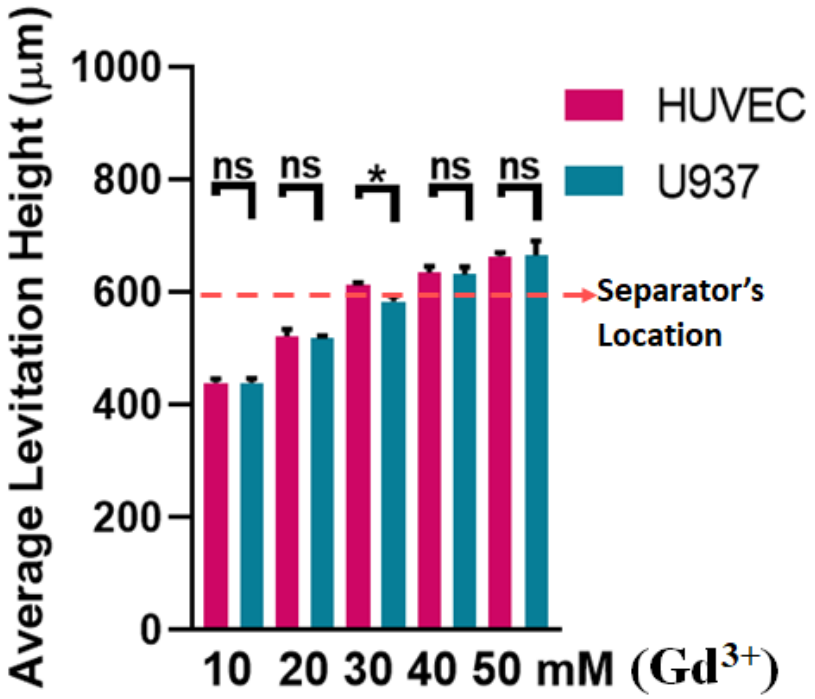

Figure 2.9. The graph of average levitation heights of HUVECs and U937 Cells in PDMS microfluidic chip.

A significant difference in levitation height was observed at 30 mM Gd^{3+} concentration. However, this concentration alone was insufficient to effectively separate HUVECs from U937 cells. Consequently, the flow ratio was adjusted. The channel width is 400 µm, and various flow ratios were tested.

2.3.3. Magnetic Levitation-based HUVEC and U937 Cells Sorting in PDMS Microfluidic Chip

For sorting experiments using the underflow method, the following cell numbers were used: 10^3 cells per mL for HUVECs and 10^6 cells per mL for U937 cells. In the first trial, the overall flow rate was set to 1 mL/h. Using the withdrawal method, the top and bottom flow rates were set at 0.5 mL/h, and the cells were sorted separately. After sorting,

the cells were counted and the calculation of sorting efficiency was done with the help of Equation 2.1:

$$Sorting\ Efficiency\ for\ HUVECs = \frac{Top_{HUVECs}}{Top_{HUVECs} + Bottom_{HUVECs}} \quad (2.1)$$

, where Top_{HUVECs} and $Bottom_{HUVECs}$ represent the number of HUVECs counted from the top and bottom outlets, respectively. The same equation was used for U937 cells as well.

The sorting efficiency for HUVECs was 20.22 ± 2.65% and for U937 cells, it was 33.73 ± 3.13% from the top outlet (Figure 2.10). After adjusting the flow rate ratios for the top and bottom outlets to 0.55 mL/h and 0.45 mL/h, respectively, the cells were counted again, and sorting efficiency was recalculated. The sorting efficiency for HUVECs increased to 23.13 ± 2.76%, and for U937 cells, it was 30.17 ± 3.32% from the top outlet (Figure 2.10). Although there was a slight improvement in sorting efficiencies, these results did not meet the study's aim, as the cells needed more time to levitate in the chip before exiting through the respective outlets.[32] Therefore, the total flow rate was adjusted to 0.4 mL/h (Figure 2.10). While the sorting efficiency improved slightly, it still required further adjustment. Consequently, the flow rate was set to 0.2 mL/h, with various ratios of top to bottom outlets, including 3:1, 2.5:1.5, 3:2, and 2:1 (Figure 2.11).

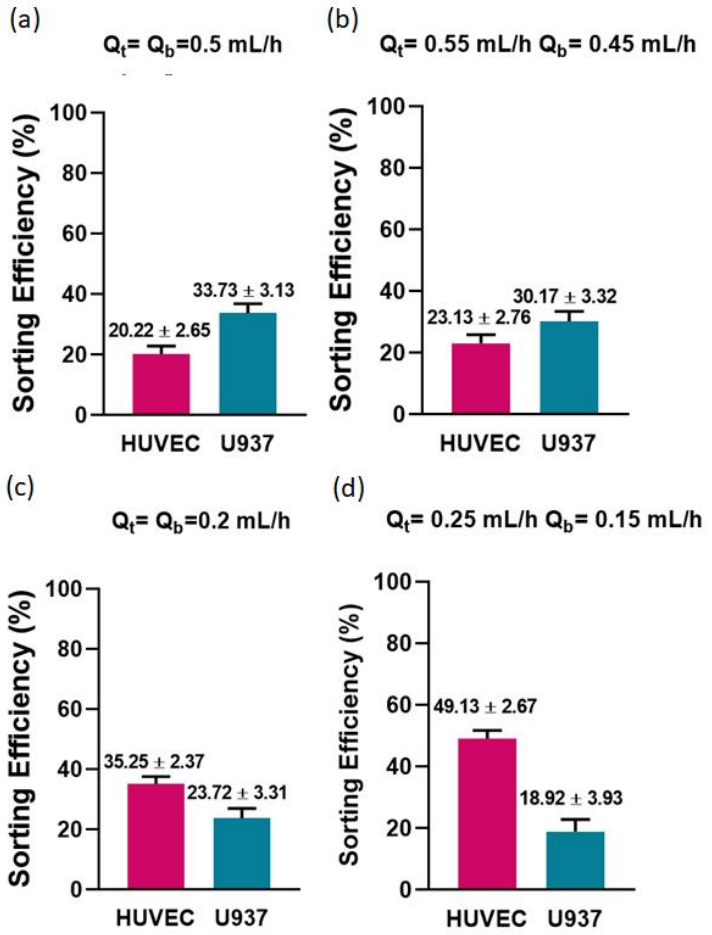

Figure 2.10. The graph of the sorting efficiencies at the top outlet for 10^3 cells/mL HUVECs and 10^6 cells/mL U937 cells under a 30 mM Gd^{3+} concentration, (a) and (b) with a total withdrawal rate of 1 mL/h, and (c) and (d) with a total withdrawal rate of 0.4 mL/h.

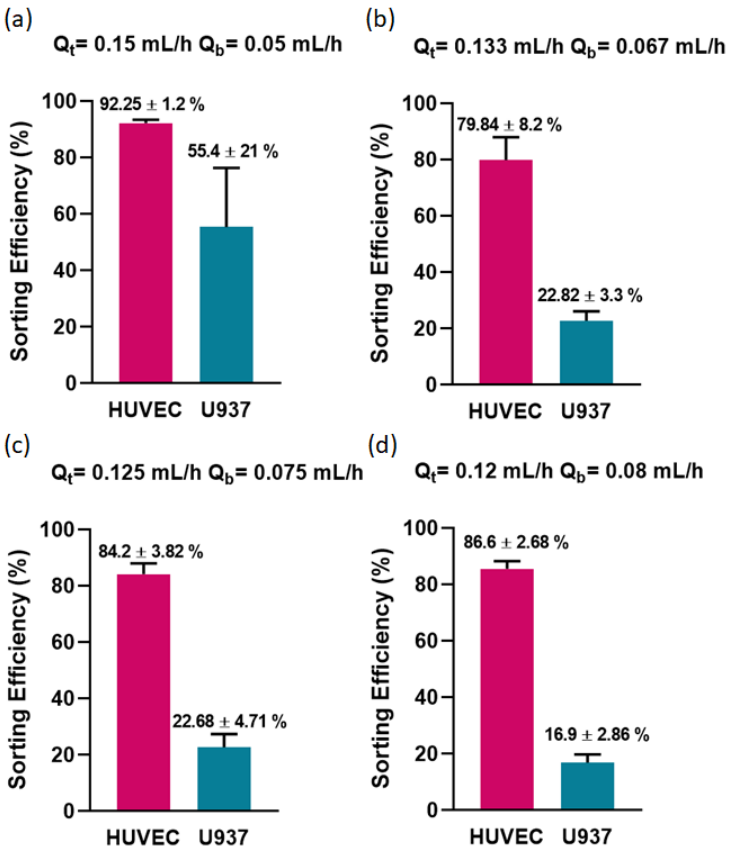

Figure 2.11. The graph of the sorting efficiencies at the top outlet for 10^3 cells/mL HUVECs and 10^6 cells/mL U937 cells under a 30 mM Gd^{3+} concentration with a total withdrawal rate of 0.2 mL/h using (a) 3:1, (b) 2:1, (c) 2.5:1.5, and (d) 3:2 ratios from the top and bottom outlets.

The sorting efficiency of HUVECs improved with the adjusted flow rate, and by changing the flow rate ratio between the top and bottom withdrawal rates, the purity of the sorted cells could be enhanced. After optimizing the sorting conditions for the individual cell types, a mixture of 10^3 HUVECs/mL and 10^6 U937 cells/mL was sorted at a Gd^{3+} concentration of 30 mM (Figure 2.12). Although there were slight changes in sorting efficiencies, likely due to the increased overall cell concentrations, these adjustments demonstrated that this system can be effectively used for endothelial cell sorting applications. When the flow rates were set to 0.12 mL/h for the top outlet and 0.08 mL/h for the bottom outlet, the sorting efficiencies were 86.67 ± 10.4% for HUVECs and

20.83 ± 8.93% for U937 cells from the top outlet (Figure 2.12). These results indicate the highest efficiency and purity achieved.

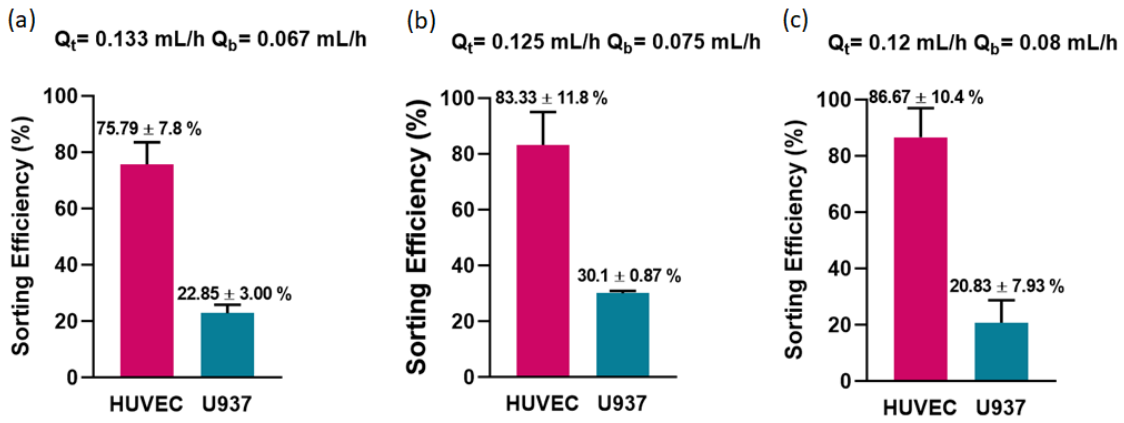

Figure 2.12. The graph of the sorting efficiencies at the top outlet for a mixture of 10^3 cells/mL HUVECs and 10^6 cells/mL U937 cells under a 30 mM Gd^{3+} concentration with a total withdrawal rate of 0.2 mL/h using (a) 2:1, (b) 2.5:1.5, and (c) 3:2 ratios from the top and bottom outlets.

2.4. Conclusion

In conclusion, HUVEC cell sorting was performed with 10^3 HUVECs/mL and 10^6 U937 cells/mL under a 30 mM Gd^{3+} concentration with various withdrawal rates. Initially, with an overall flow rate of 1 mL/h, the top and the bottom flow rate were set at 0.5 mL/h and the sorting efficiency for HUVECs was 20.22 ± 2.65%, and for U937 cells, it was 33.73 ± 3.13%. These results did not meet the study's aim, so the flow rates were decreased first to 0.4 mL/h and then further to 0.2 mL/h. At a total flow rate of 0.2 mL/h, the sorting efficiencies significantly improved, ranging between 79-94% for HUVECs, across different flow rate ratios of 3:1, 2:1, 2.5:1.5, and 3:2. This demonstrated that adjusting the flow rate improved sorting efficiency, with the best results obtained after fine-tuning the flow rate. When cells were mixed and introduced to the system, the sorting efficiencies were consistent, showing 75.79 ± 7.8%, 83.33 ± 11.8%, and 86.67 ± 10.4%

for HUVECs and 22.85 ± 3%, 30.1 ± 0.87%, and 20.83 ± 7.93% for U937 cells at the top outlet. The highest efficiency and purity were achieved with flow rates of 0.12 mL/h for the top outlet and 0.08 mL/h for the bottom outlet.

CHAPTER 3

MAGNETIC LEVITATION-BASED LIVE-DEAD CELL SORTING

In this chapter, MagLev technology is used for live-dead sorting of MDA-MB-231 breast cancer cells. It begins with an overview of the current state of live cell enrichment and its importance. Next, the designed experiments for live cell sorting and their suitability for 3D cell culture applications are presented. Finally, all results are given and discussed.

3.1. State of the Art Circulating Endothelial Cell Sorting in Microfluidic Devices

The separation or enrichment of live cells is crucial for tissue engineering applications, drug screening, and testing studies, as viable cells are essential in these fields.[51] In tissue engineering, live cell sorting is vital for obtaining only viable cells to increase the success rate in applications such as stem cell grafts, stem cell transplants, and neurological regenerative therapy.[32,52] Conventional methods for live cell sorting, such as FACS and MACS, involve labeling steps that increase costs and the risk of false positive results from nonspecific reagent binding.[53] Consequently, scientists are turning to label-free microfluidic techniques.

A novel label-free microfluidic approach was developed in live and dead cell sorting based on stiffness differences (Figure 3.1).[54] The microfluidic chip has three inlets and outlets. The middle inlet is for the cell mixture, while the top and bottom inlets are for the flow. The top outlet collects the stiffer, nonviable cells, the middle outlet collects

a mixture of live and dead cells, and the bottom outlet collects the less stiff, viable cells. The microfluidic chip achieves separation using a channel with repeated diagonal ridges.

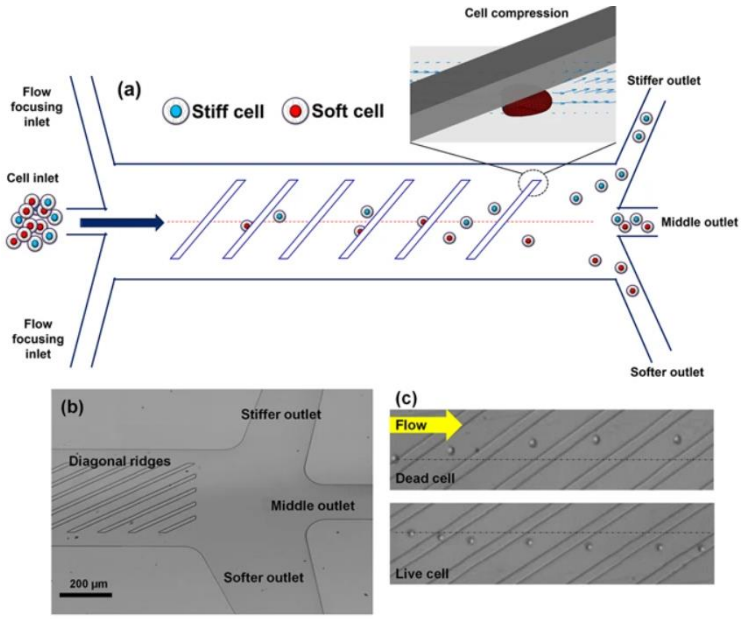

Figure 3.1. Illustration of a ridge-based microfluidic device for sorting of live cells. (a) Cells directed through ridges and flow toward different outlets depending on the difference in stiffness. (b) A close-up of the ridges and outlets with an optical micrograph. (c) A close-up of the flow of live and dead cells.[54]

A novel magnetic levitation-based label-free sorting device called CelLEVITAS was developed for live and dead cells.[55] It consists of a flow channel that is 1 mm high and 1 mm wide. Positioned between two magnets, it separates live cells depending on their magnetic and density properties. A withdrawal flow is employed for the separation process. After separation, dead cells and debris are collected at the bottom outlet, while live cells are sorted at the top outlet.

The aim of this study is to highlight the importance of obtaining viable cells for cell enrichment purposes without using expensive labeling methods. MagLev principles and the density difference between live and dead cells were utilized for this purpose. After sorting live cells from dead ones, the cells collected from the top outlet were tested for their suitability in 3D cell culture applications. The hanging drop method was used to

create spheroids, which were then subjected to drug treatment and observed under the MagLev principle. Consequently, the technology developed in this thesis will have various applications in medicine.

3.2. Materials and Methods

The MagLev technology and platform discussed in Chapter 2 were also used in this chapter.

3.2.1. Cell Culture

MDA-MB-231 breast cancer cells were cultured in Dulbecco's Modified Eagle Medium high glucose (DMEM, Gibco), supplemented with 1% Penicillin-Streptomycin and 10% FBS.[56] The cells were maintained in an incubator at 37°C with 5% CO_2. Once the cells reached the desired growth stage, they were prepared for experiments.

To prepare the cells, the supernatant from the MDA-MB-231 culture was discarded, and Trypsin-EDTA (Euroclone) was added to detach the cells.[56] Detachment was carried out at 37°C for 10 minutes, followed by centrifugation for 5 minutes at 1200 rpm. The remaining cells were resuspended in 1 mL of DMEM, and the desired cell concentration was used for experiments.

For preparing dead cells, the resuspended cells in 1 mL of DMEM were treated with DMSO (Isolab) for one hour at 37°C. After this treatment, the cells were centrifuged for 5 minutes at 1200 rpm, the supernatant was discarded, and the cells were resuspended in 1 mL of DMEM. The desired cell concentration was then used for the experiment.

3.2.2. Hanging Drop Technique and Drug Treatment

For the hanging drop procedure, cells were taken separately from the top and bottom outlets after a 1:1 ratio of mixed Live and Dead MDA-MB-231 cell sorting. The cell mixture was centrifuged for 5 minutes at 1200 rpm, the supernatant was discarded, and the cells were resuspended in DMEM. Each hanging drop contained 10 µL of the cell mixture.[56] Images were taken at a time of 0, 24, 48, 72, and 96 hours to compare spheroid formation parameters, including time and diameter. After achieving compact spheroid formation, the spheroids were gently transferred to the MagLev platform and placed in the capillary channel under conditions of 100 mM hydrochloric acid (HCl) and 50 mM Gd^{3+}.

3.3. Results and Discussion

3.3.1. Magnetic Levitation of Live and Dead MDA-MB-231 Cells Static Condition in PDMS Microfluidic Chip

For sorting experiments under static conditions in the PDMS microfluidic device, MDA-MB-231 cells were used at a concentration of 10^4 cells/mL. These cells were analyzed separately under static conditions to determine the optimum average levitation height difference. After cell calculation, a paramagnetic medium with different concentrations of 50, 60, 75, and 100 mM Gd^{3+} was added to the solution. Prepared solutions of 20 µL were loaded into the microfluidic chip. Following 15 minutes, the images were captured at 5× magnification using an inverted microscope (Zeiss Axio Vert A1, Germany) (Figure 3.2).

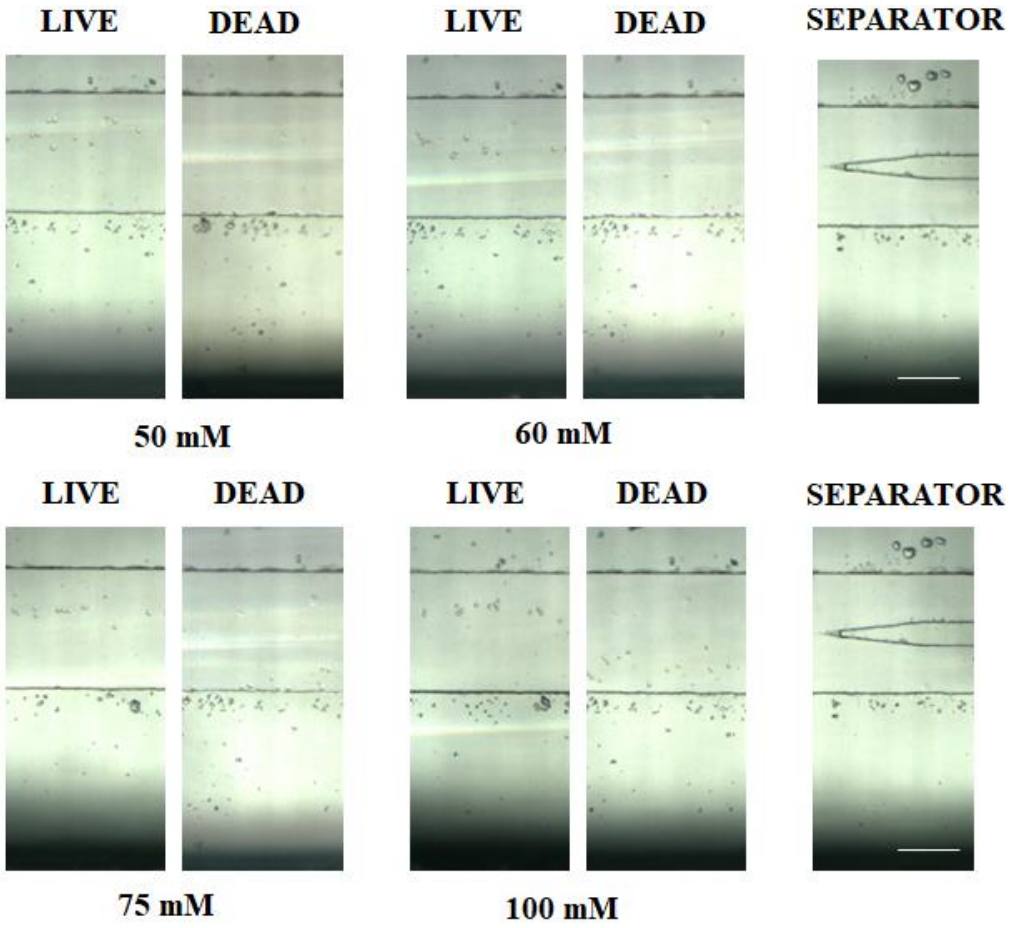

Figure 3.2. The micrographs of levitated MDA-MB-231 cells with varying Gd^{3+} concentrations of 50, 60, 75, and 100 mM. Scale Bar indicates 200 μm.

The levitation height of cells in the MagLev platform was assessed using the ImageJ program. The distance from the bottom magnet to the center of each cell was measured. For all concentrations and cell types, average levitation heights were calculated, and t-tests were conducted (Figure 3.3). The average levitation heights of live and dead MDA-MB-231 cells were found to be significantly different across all Gd^{3+} concentrations. Additionally, it was observed that an increase in the paramagnetic medium concentration resulted in a higher levitation height. These results indicate that the choice of Gd^{3+} concentration may vary depending on the application. Using a low Gd^{3+} concentration is important to achieve the maximum difference in average levitation height between the live and dead cells. These findings have the potential to be applied in sorting endothelial cells using the MagLev principle.

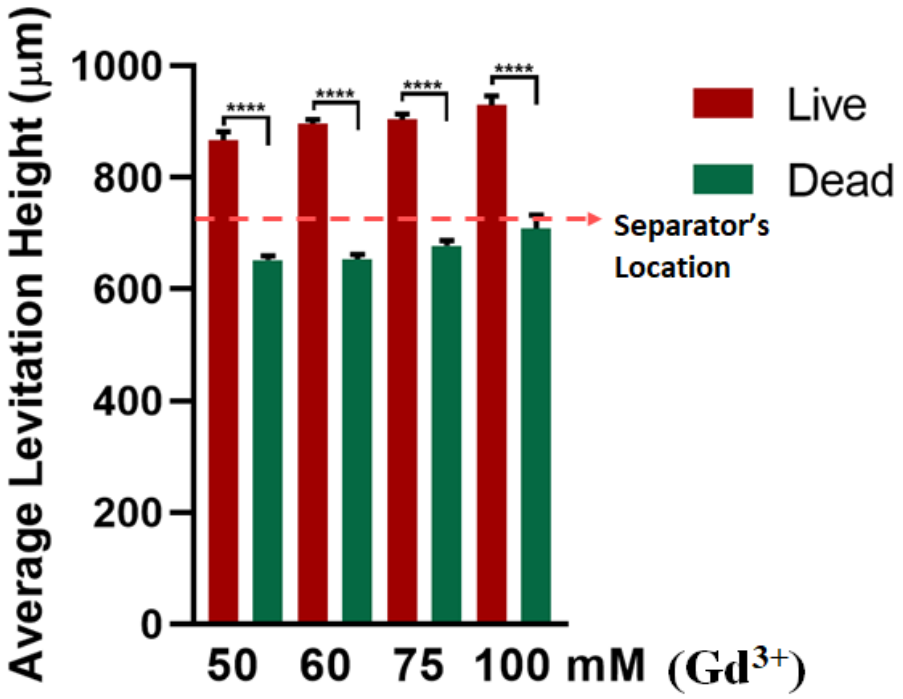

Figure 3.3. The graph of average levitation heights of live and dead MDA-MB-231 Cells

3.3.2. Magnetic Levitation of Live and Dead MDA-MB-231 Cells Sorting in PDMS Microfluidic Chip

For sorting experiments using the underflow method, the following cell numbers were used: 10^6 cells/mL for both live and dead MDA-MB-231 cells under 75 mM Gd^{3+} conditions. In the first trial, the overall flow rate was set to 1 mL/h. Using the withdrawal method, the top and bottom flow rates were each set at 0.5 mL/h. In this experiment, live and dead MDA-MB-231 cells were sorted separately. After sorting, the cells were counted and the calculation of sorting efficiency was done. The sorting efficiency for live cells was 65.67 ± 9%, and for dead cells, it was 21.34 ± 4.82% (Figure 3.4). These results did not meet the study's aim, as the cells needed more time to levitate in the chip before exiting through the respective outlets.[32] Therefore, the total flow rate was subsequently adjusted to 0.5 mL/h (Figure 3.4). While the sorting efficiency improved slightly, further adjustment was needed. Therefore, the flow rate was set to 0.25 mL/h, similar to the adjustment made in CEC sorting (Figure 3.4).

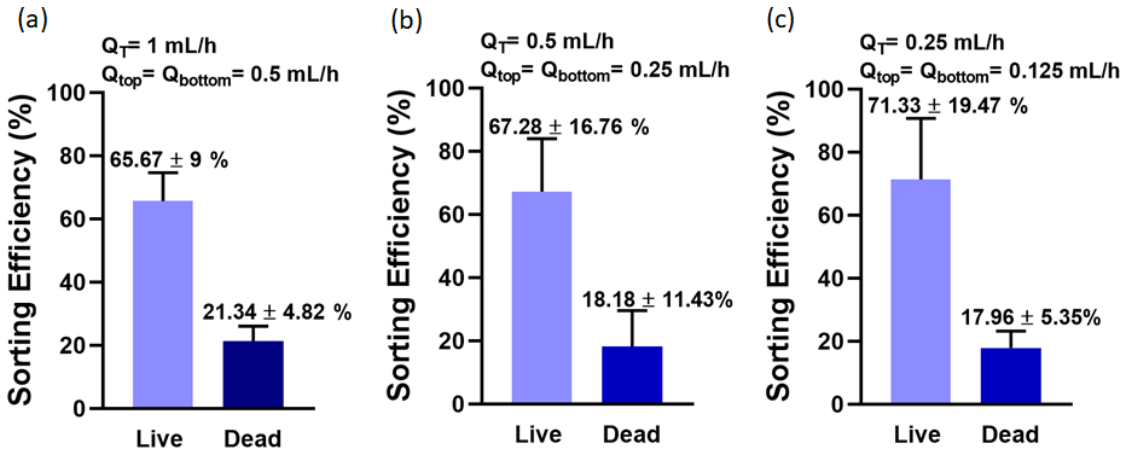

Figure 3.4. The graph of the sorting efficiencies at the top outlet for both 10^6 cells/mL live and dead MDA-MB-231 cells under a 75 mM Gd^{3+} concentration with a total withdrawal rate of (a) 1 mL/h, (b) 0.5 mL/h, (c) 0.25 mL/h.

The sorting efficiency of live MDA-MB-231 cells improved with an adjusted total flow rate of 0.5 mL/h. By altering the flow rate ratio between the top and bottom withdrawal rates, the purity of the sorted cells was enhanced (Figure 3.5). However, these results were still not as good as those obtained with a total flow rate of 0.25 mL/h. Thus, the total flow rate was set to 0.25 mL/h, with adjustments to the flow rate ratios (Figure 3.6). When the flow rates were set equal to 0.125 mL/h the sorting efficiencies were 71.33 ± 19.47% for live and 17.96 ± 5.35% for dead cells from the top outlet. However, when the flow rate ratios changed and set to 0.1 mL/h for the top outlet and 0.15 mL/h for the bottom outlet, the sorting efficiencies were 86.03 ± 2.54% for live and 6.21 ± 1.46% for dead MDA-MB-231 cells from the top outlet (Figure 3.6).

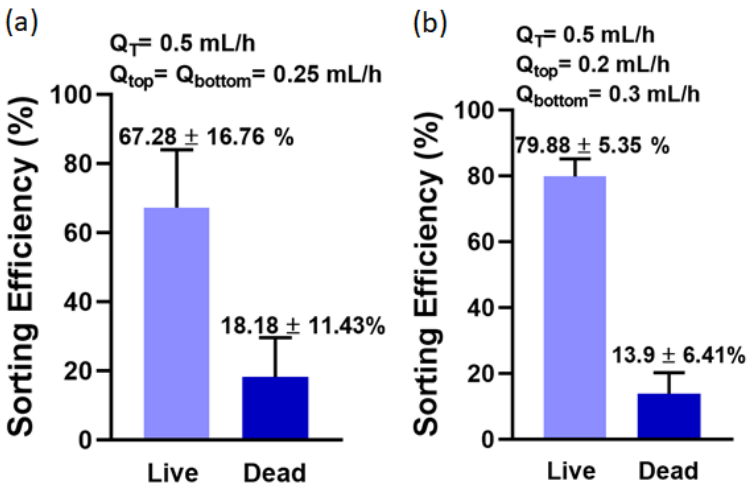

Figure 3.5. The graph of the sorting efficiencies at the top outlet for both 10^6 cells/mL live and dead MDA-MB-231 cells under a 75 mM Gd^{3+} concentration with a total withdrawal rate of 0.5 mL/h using (a) 1:1, and (b) 1:1.5 ratios.

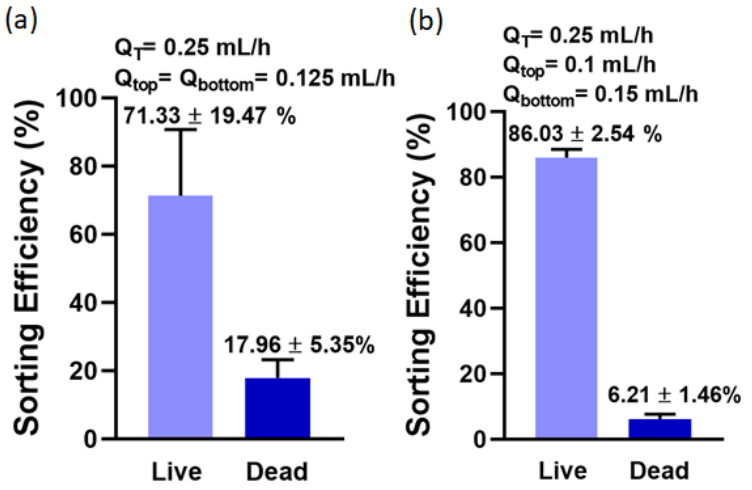

Figure 3.6. The graph of the sorting efficiencies at the top outlet for both 10^6 cells/mL live and dead MDA-MB-231 cells under a 75 mM Gd^{3+} concentration with a total withdrawal rate of 0.25 mL/h using (a) 1:1 and, (b) 1:1.5 ratios.

After optimizing the sorting conditions for individual cell types, a mixture of 10^6 MDA-MB-231 cells/mL was sorted at a Gd^{3+} concentration of 75 mM with flow rates of 0.1 mL/h and 0.15 mL/h from the top and bottom outlets, respectively (Figure 3.7). To further improve the sorting efficiency difference between live and dead cells, a flow ratio of 1:4 was tested (Figure 3.7). Although there were slight changes in sorting efficiencies, likely due to increased overall cell concentrations, these adjustments demonstrated that this system can be effectively used for live cell sorting applications. When the flow rates were set to 0.1 mL/h for the top outlet and 0.15 mL/h for the bottom outlet, the sorting efficiencies were 77.87 ± 9.82% for live cells and 11.02 ± 5.81% for dead cells from the top outlet (Figure 3.7). These results indicate the highest efficiency achieved.

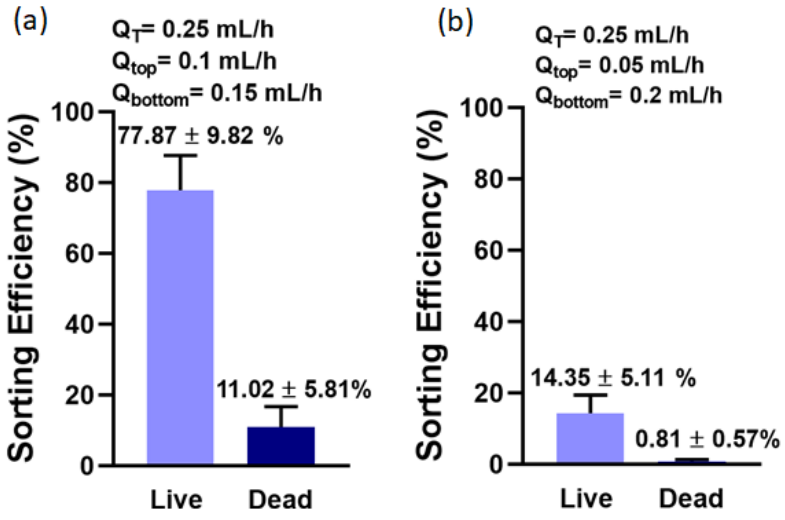

Figure 3.7. The sorting efficiencies of live and dead MDA-MB-231 cells at the top outlet for a mixture of both 10^6 cells/mL under a 75 mM Gd^{3+} concentration with a total withdrawal rate of 0.25 mL/h using (a) 1:1.5, and (b) 1:4 ratios.

3.3.3. 3D Cell Culture with Hanging Drop Method

After sorting, the cells collected from the top and bottom outlets were used to form spheroids using the hanging drop method to observe any differences due to varying flow

rates. The spheroid formations were observed under the following conditions: a total withdrawal rate of 0.25 mL/h for only live cells (Figures 3.8 and 3.9) and a control group without sorting of live cells (Figure 3.10).

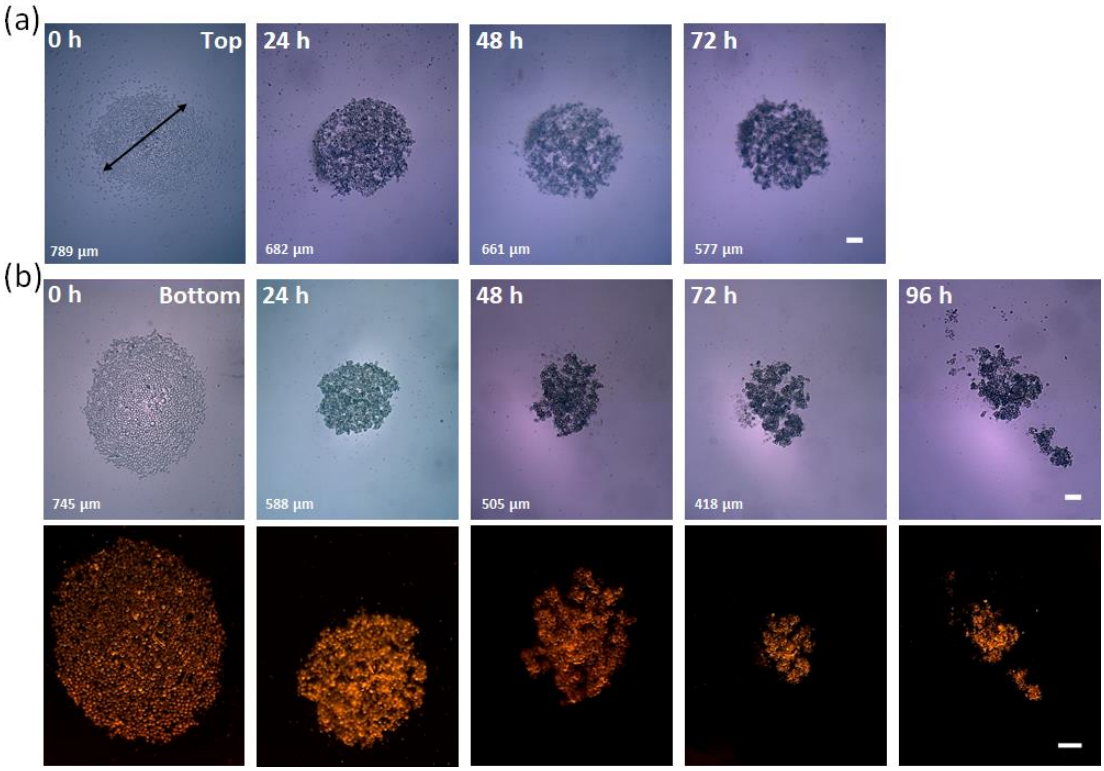

Figure 3.8. Micrographs of MDA-MB-231 cell spheroids containing only live cells after sorting with a withdrawal rate of 0.125 mL/h in a ratio of 1:1 under 75 mM Gd^{3+} concentration. Brightfield and fluorescent images show spheroid formations of cells collected from (a) top and (b) bottom outlets. Scale Bar indicates 200 µm.

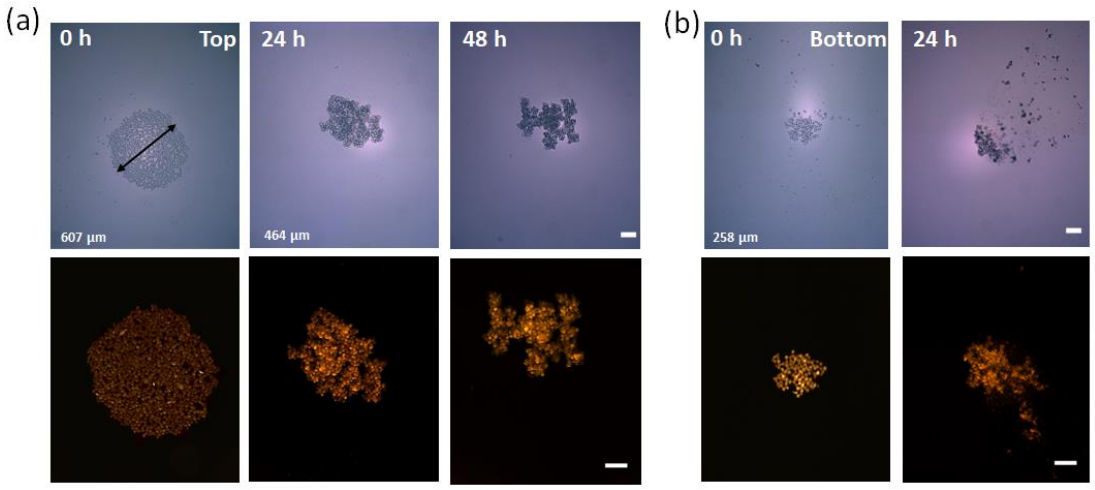

Figure 3.9. Micrographs of MDA-MB-231 cell spheroids containing only live cells after sorting with a withdrawal rate of 0.1 mL/h and 0.15 mL/h from top and bottom outlets in a ratio of 1:1.5 under 75 mM Gd^{3+} concentration. Brightfield and fluorescent images show spheroid formations of cells collected from (a) top and (b) bottom outlets. Scale Bar indicates 200 µm.

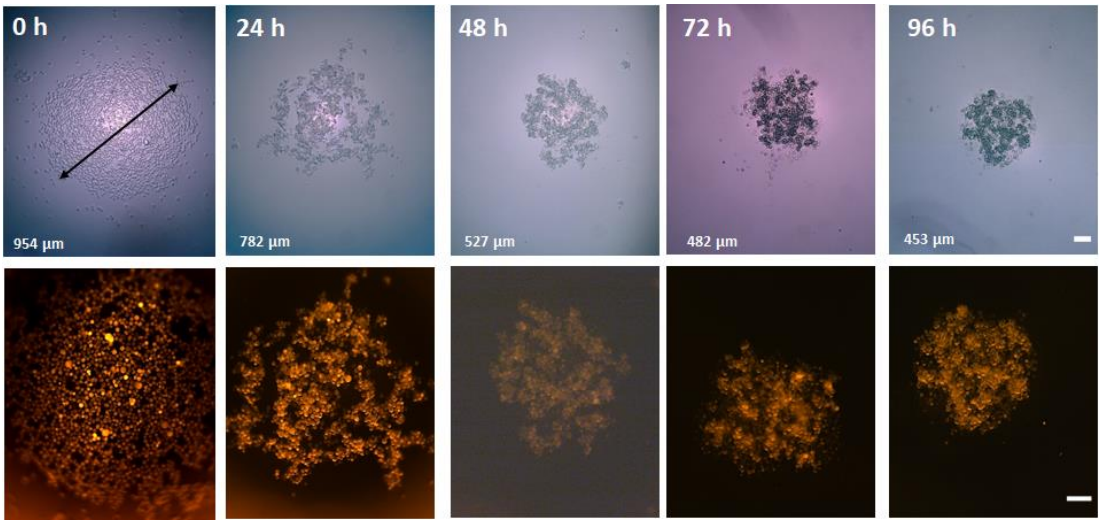

Figure 3.10. Brightfield and fluorescent micrographs of MDA-MB-231 cell spheroids containing only live cells before sorting. Scale Bar indicates 200 µm.

The comparison of the spheroids was done using diameters (Figure 3.11). When the spheroids were made from cells sorted from the top outlet, their diameters were 789 µm at 0 hours and 557 µm at 72 hours. In contrast, the spheroids made from unsorted cells had diameters of 954 µm at 0 hours and 482 µm at 72 hours. It was observed that before sorting, the spheroid diameters were comparable to or larger than those formed after sorting (Figure 3.11).

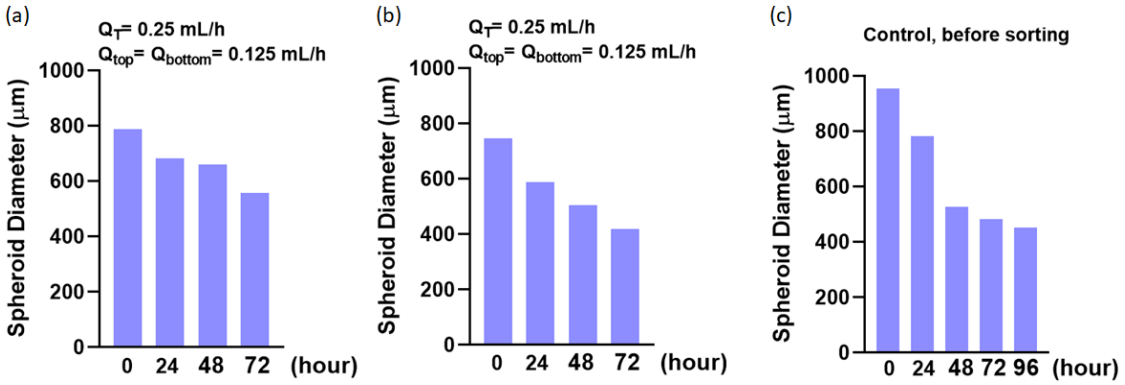

Figure 3.11. Graphs showing the change in spheroid diameters of MDA-MB-231 cells over time. The spheroid diameters are presented for sorted cells collected from (a) top and (b) bottom outlets and (c) for unsorted cells.

The cell clusters were then subjected to HCl treatment using MagLev after achieving a compact structure (Figures 3.12 and 3.13). These clusters were made from the sorting of cells collected from the top and bottom outlets. The HCl treatment was applied to the clusters, and the change in levitation heights was observed (Figure 3.14). After 30-40 minutes of HCl treatment, the clusters no longer levitated. The clusters were then dyed with trypan blue to confirm that all the cells were dead. As a control, clusters were also placed into the capillary without any HCl treatment, and they did not change their levitation height even after 3 hours.

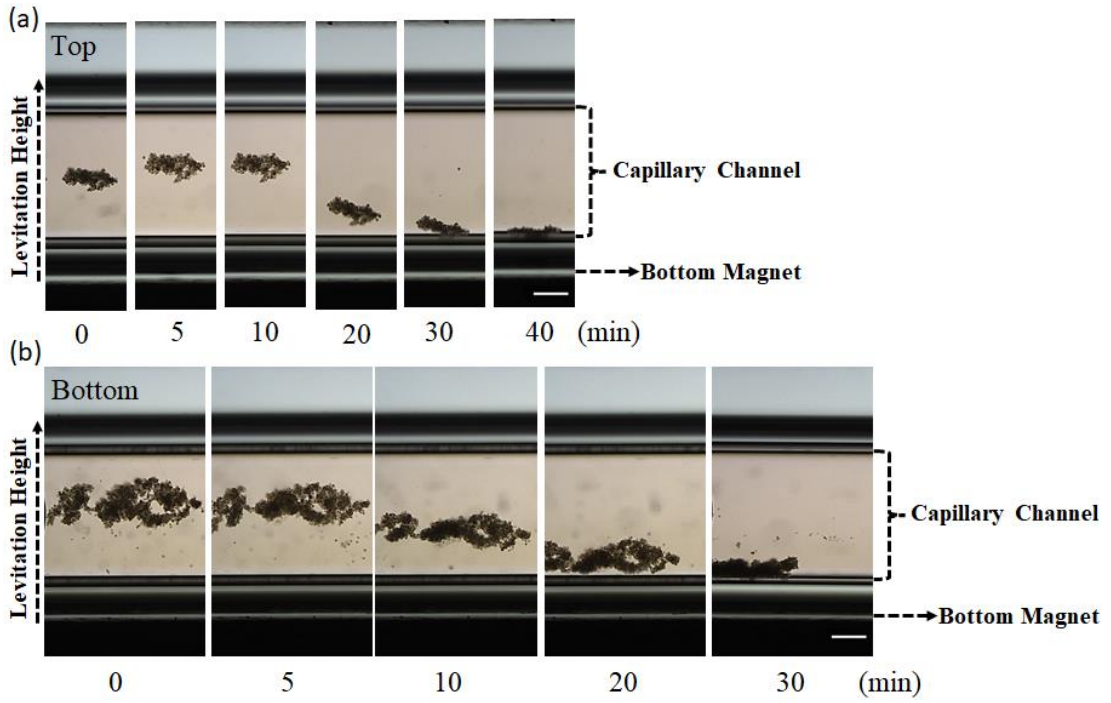

Figure 3.12. Micrographs of levitated MDA-MB-231 cell clusters under HCl treatment. 3D cell clusters were achieved for cells collected from (a) top and (b) bottom outlets of the magnetic levitation platform. Scale Bar indicates 200 μm.

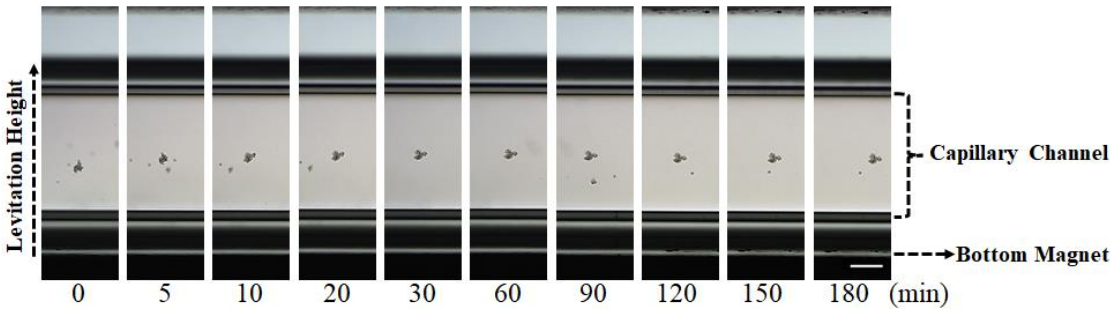

Figure 3.13. Micrographs of levitated MDA-MB-231 cell clusters without HCl treatment as a control group. Scale Bar indicates 200 μm.

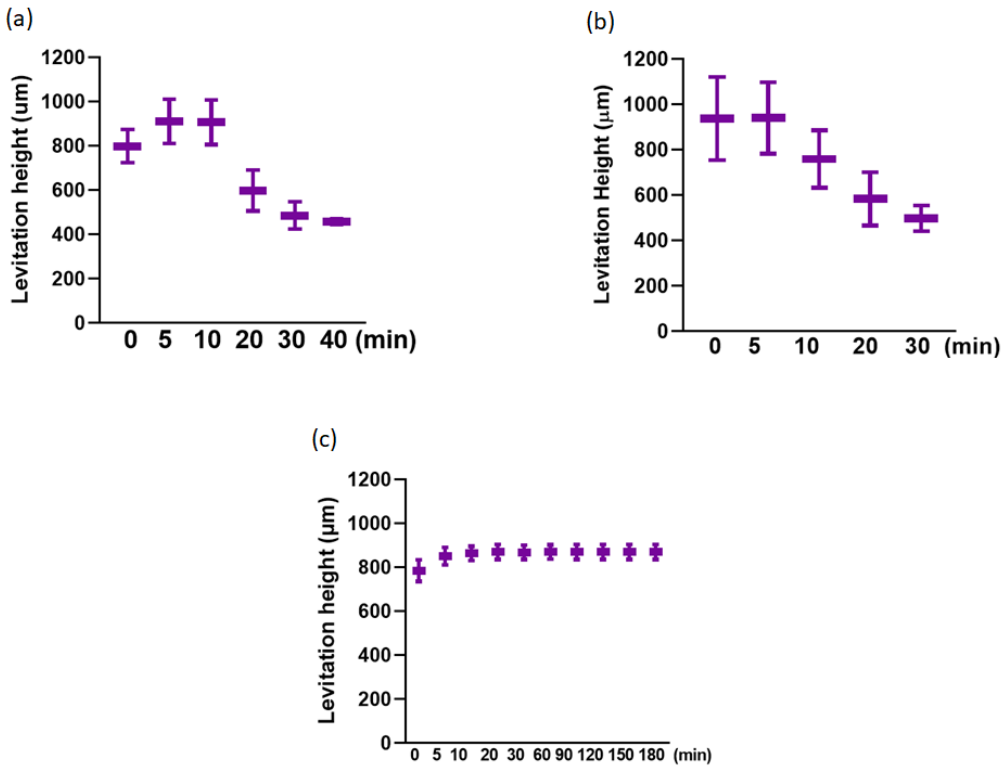

Figure 3.14. Graphs illustrating the changes in levitation heights of MDA-MB-231 cell clusters. 3D cell clusters were formed from cells collected from the magnetic levitation platform's (a, c) top and (b) bottom outlets. The clusters were levitated (a, b) with HCl and (c) without HCl.

3.4. Conclusion

In conclusion, live-dead MDA-MB-231 cell sorting was performed with both live and dead 10^6 MDA-MB-231 cells/mL under a 75 mM Gd^{3+} concentration with various withdrawal rates. Initially, with an overall flow rate of 1 mL/h, both the top and bottom outlet flow rates were set at 0.5 mL/h. The sorting efficiency for live MDA-MB-231 cells was 65.67 ± 9%, and for dead MDA-MB-231 cells, it was 21.34 ± 4.82%. These results did not meet the study's aim, so the flow rates were decreased first to 0.5 mL/h and then further to 0.25 mL/h. At a total flow rate of 0.25 mL/h, the sorting efficiencies significantly improved, ranging between 71-86% for live MDA-MB-231 cells, across different flow rate ratios of 1:1 and 1:1.5. This demonstrated that adjusting the flow rate

improved sorting efficiency, with the best results obtained after fine-tuning the flow rate. When cells were mixed and introduced to the system, the sorting efficiencies were consistent, showing 77.87 ± 9.82% for live MDA-MB-231 cells, and 11.02 ± 5.81% for dead MDA-MB-231 cells at the top outlet. The highest efficiency was achieved with flow rates of 0.1 mL/h for the top outlet and 0.15 mL/h for the bottom outlet.

After sorting the live cells, they were used for 3D cell culture using the hanging drop method to form spheroids. The sorted cells showed an immediate diameter decrease compared to the control group, which was not sorted. After achieving compact spheroid formation, these clusters were treated with HCl, and their levitation height decrease was observed over time. This indicates the cells inside spheroids are dying with HCl treatment, which can be observed with the levitation height changes of clusters.

CHAPTER 4

CONCLUSIONS

Cardiovascular diseases are the leading cause of death, accounting for more than 90% of fatalities. CECs, which are mature endothelial cells, can serve as biomarkers for cardiovascular diseases. Despite the challenges in sorting CECs, such as their low numbers, they are crucial for diagnostic purposes. Traditional techniques for sorting CECs often rely on labels or general immunomagnetic and immunofluorescent markers.

In this study, the magnetic levitation principle was utilized due to its advantages in terms of simplicity, cost-effectiveness, and reduced risk compared to methods like FACS and MACS, which can adversely affect cell viability. The developed magnetic levitation platform demonstrated high sorting efficiency, achieving 86.67% for endothelial cells (HUVECs) at a concentration of 10^3 cells/mL using 30 mM Gadavist under a flow rate of 0.2 mL/h.

As a result of this study, circulating endothelial cells (CECs) were successfully sorted on a microfluidic chip for the first time, using only their unique density as a biomarker to distinguish them from white blood cells (WBCs). Additionally, a novel approach was introduced by creating a virtual separator through the manipulation of flow rate ratios between the top and bottom outlets, enhancing the sorting process. This innovation marks a significant advancement in the use of microfluidic technology for precise cell separation. The developed magnetic levitation platform offers a rapid, low-cost, and label-free in-vitro diagnostic method for cardiovascular diseases by sorting CECs from whole blood with high throughput and purity. The sorted cells can also be collected for downstream analysis in personalized medicine.

Another aspect of this study focused on the live-dead sorting of breast cancer cells for spheroid formation. The methodology demonstrates that this system is effective for live/dead cell separation. Following the separation, spheroid formation can be achieved using the hanging drop method. After spheroid formation, the cells were treated with HCl

to observe changes in their levitation behavior. Following 45 minutes of HCl treatment, all structured cancer cell clusters were dyed, indicating no levitation due to their high densities. This absence of levitation suggests that this method could potentially be used for treatment applications.

In this thesis, a novel microfluidic sorting system based on magnetic levitation principles has been developed, achieving high efficiency in separating circulating endothelial cells (CECs) from white blood cells (WBCs) and live cancer cells from dead ones with the help of creating virtual separator. This label-free and cost-effective method demonstrates significant potential for cell sorting. For future studies, this chip can be applied to different cell lines and integrated with lab-on-a-chip devices to enable further cell analysis. The results highlight the system's potential applications in the early detection of cardiovascular diseases, tissue engineering, and personalized medicine. We are enthusiastic about the prospects and the ongoing contributions this research will make to the scientific and medical communities.

REFERENCES

1. Yousuff, C.; Ho, E.; Hussain K., I.; Hamid, N. Microfluidic Platform for Cell Isolation and Manipulation Based on Cell Properties. *Micromachines (Basel)* **2017**, *8* (1), 15. https://doi.org/10.3390/mi8010015.

2. Hider, R. Differential White Cell Counts: An e-Learning Resource. *Bioscience Horizons* **2010**, *3* (1), 10–20. https://doi.org/10.1093/biohorizons/hzq003.

3. Lu, N.; Tay, H. M.; Petchakup, C.; He, L.; Gong, L.; Maw, K. K.; Leong, S. Y.; Lok, W. W.; Ong, H. B.; Guo, R.; Li, K. H. H.; Hou, H. W. Label-Free Microfluidic Cell Sorting and Detection for Rapid Blood Analysis. *Lab Chip* **2023**, *23* (5), 1226–1257. https://doi.org/10.1039/D2LC00904H.

4. Sutermaster, B. A.; Darling, E. M. Considerations for High-Yield, High-Throughput Cell Enrichment: Fluorescence versus Magnetic Sorting. *Sci Rep* **2019**, *9* (1), 227. https://doi.org/10.1038/s41598-018-36698-1.

5. Witek, M. A.; Freed, I. M.; Soper, S. A. Cell Separations and Sorting. *Anal Chem* **2020**, *92* (1), 105–131. https://doi.org/10.1021/acs.analchem.9b05357.

6. Kecili, S.; Yilmaz, E.; Ozcelik, O. S.; Anil-Inevi, M.; Gunyuz, Z. E.; Yalcin-Ozuysal, O.; Ozcivici, E.; Tekin, H. C. MDACS Platform: A Hybrid Microfluidic Platform Using Magnetic Levitation Technique and Integrating Magnetic, Gravitational, and Drag Forces for Density-Based Rare Cancer Cell Sorting. Biosens *Bioelectron X* **2023**, *15* (1), 100392. https://doi.org/10.1016/j.biosx.2023.100392.

7. Ozcan, H. A.; Kecili, S.; Tekin, H. C. Magnetic Levitation-Based Endothelial Cell Sorting. In 2023 Medical Technologies Congress (TIPTEKNO); *IEEE*, **2023**; pp 1–4. https://doi.org/10.1109/TIPTEKNO59875.2023.10359216.

8. Buryk-Iggers, S.; Kieda, J.; Tsai, S. S. H. Diamagnetic Droplet Microfluidics Applied to Single-Cell Sorting. *AIP Adv* **2019**, *9* (7), 075106. https://doi.org/10.1063/1.5095884.

9. Erdbruegger, U.; Haubitz, M.; Woywodt, A. Circulating Endothelial Cells: A Novel Marker of Endothelial Damage. *Clinica Chimica Acta* **2006**, *373* (1–2), 17–26. https://doi.org/10.1016/j.cca.2006.05.016.

10. Woywodt, A. Circulating Endothelial Cells: Life, Death, Detachment and Repair of the Endothelial Cell Layer. *Nephrology Dialysis Transplantation* **2002**, *17* (10), 1728–1730. https://doi.org/10.1093/ndt/17.10.1728.

11. Yu, H.-K.; Lee, H.-J.; Choi, H.-N.; Ahn, J.-H.; Choi, J.-Y.; Song, H.-S.; Lee, K.-H.; Yoon, Y.; Yi, L. S. H.; Kim, J.-S.; Kim, S. J.; Kim, T. J. Characterization of CD45−/CD31+/CD105+ Circulating Cells in the Peripheral Blood of Patients with Gynecologic Malignancies. *Clinical Cancer Research* **2013**, *19* (19), 5340–5350. https://doi.org/10.1158/1078-0432.CCR-12-3685.

12. Carter, A. D.; Bonyadi, R.; Gifford, M. L. The Use of Fluorescence-Activated Cell Sorting in Studying Plant Development and Environmental Responses. *Int J Dev Biol* **2013**, *57* (6-7–8), 545–552. https://doi.org/10.1387/ijdb.130195mg.

13. Bonner, W. A.; Hulett, H. R.; Sweet, R. G.; Herzenberg, L. A. Fluorescence Activated Cell Sorting. Review of *Scientific Instruments* **1972**, *43* (3), 404–409. https://doi.org/10.1063/1.1685647.

14. Galbraith, D. W. Flow Cytometry and Fluorescence-Activated Cell Sorting in Plants: The Past, Present, and Future. *Biomédica* **2012**, *30* (0), 65. https://doi.org/10.7705/biomedica.v30i0.824.

15. Hodne, K.; Weltzien, F.-A. Single-Cell Isolation and Gene Analysis: Pitfalls and Possibilities. *Int J Mol Sci* **2015**, *16* (11), 26832–26849. https://doi.org/10.3390/ijms161125996.

16. Kraan, J.; Sleijfer, S.; Foekens, J. A.; Gratama, J. W. Clinical Value of Circulating Endothelial Cell Detection in Oncology. *Drug Discov Today* **2012**, *17* (13–14), 710–717. https://doi.org/10.1016/j.drudis.2012.01.011.

17. Zhang, J.; Nguyen, N.-T. Magnetic Cell Separation. In Magnetic Materials and Technologies for Medical Applications; *Elsevier*, 1st ed.; Alexander M. Tishin, 2022; pp 193–225.

18. Sun, H.; Chen, J.; Ni, B.; Yang, X.; Wu, Y. Recent Advances and Current Issues in Single-Cell Sequencing of Tumors. *Cancer Lett* **2015**, *365* (1), 1–10. https://doi.org/10.1016/j.canlet.2015.04.022.

19. ELbakry, K.; Elarabany, N.; Behery, S. Protective and Therapeutic Effects of Moringa Oleifera Against Toxicity of Lead Chloride. *Scientific Journal for Damietta Faculty of Science* **2018**, *8* (1), 11–18. https://doi.org/10.21608/sjdfs.2018.194790.

20. Wyatt Shields IV, C.; Reyes, C. D.; López, G. P. Microfluidic Cell Sorting: A Review of the Advances in the Separation of Cells from Debulking to Rare Cell Isolation. *Lab Chip* **2015**, *15* (5), 1230–1249. https://doi.org/10.1039/C4LC01246A.

21. Wu, J.; Chen, Q.; Lin, J.-M. Microfluidic Technologies in Cell Isolation and Analysis for Biomedical Applications. *Analyst* **2017**, *142* (3), 421–441. https://doi.org/10.1039/C6AN01939K.

22. Sivaramakrishnan, M.; Kothandan, R.; Govindarajan, D. K.; Meganathan, Y.; Kandaswamy, K. Active Microfluidic Systems for Cell Sorting and Separation. *Curr Opin Biomed Eng* **2020**, *13* (1), 60–68. https://doi.org/10.1016/j.cobme.2019.09.014.

23. Fernandez, R. E.; Rohani, A.; Farmehini, V.; Swami, N. S. Review: Microbial Analysis in Dielectrophoretic Microfluidic Systems. *Anal Chim Acta* **2017**, *966*, 11–33. https://doi.org/10.1016/j.aca.2017.02.024.

24. Mach, A. J.; Adeyiga, O. B.; Di Carlo, D. Microfluidic Sample Preparation for Diagnostic Cytopathology. *Lab Chip* **2013**, *13* (6), 1011. https://doi.org/10.1039/c2lc41104k.

25. Kim, G.-Y.; Han, J.-I.; Park, J.-K. Inertial Microfluidics-Based Cell Sorting. *Biochip J* **2018**, *12* (4), 257–267. https://doi.org/10.1007/s13206-018-2401-2.

26. Robert, D.; Pamme, N.; Conjeaud, H.; Gazeau, F.; Iles, A.; Wilhelm, C. Cell Sorting by Endocytotic Capacity in a Microfluidic Magnetophoresis Device. *Lab Chip* **2011**, *11* (11), 1902. https://doi.org/10.1039/c0lc00656d.

27. Gao, Y.; Li, W.; Pappas, D. Recent Advances in Microfluidic Cell Separations. *Analyst* **2013**, *138* (17), 4714. https://doi.org/10.1039/c3an00315a.

28. Mach, A. J.; Di Carlo, D. Continuous Scalable Blood Filtration Device Using Inertial Microfluidics. *Biotechnol Bioeng* **2010**, *107* (2), 302–311. https://doi.org/10.1002/bit.22833.

29. Wu, F.; Kong, X.; Liu, Y.; Wang, S.; Chen, Z.; Hou, X. Microfluidic-Based Isolation of Circulating Tumor Cells with High-Efficiency and High-Purity. *Chinese Chemical Letters* **2024**, *35* (8), 109754. https://doi.org/10.1016/j.cclet.2024.109754.

30. Nasiri, R.; Shamloo, A.; Ahadian, S.; Amirifar, L.; Akbari, J.; Goudie, M. J.; Lee, K.; Ashammakhi, N.; Dokmeci, M. R.; Di Carlo, D.; Khademhosseini, A. Microfluidic-Based Approaches in Targeted Cell/Particle Separation Based on Physical Properties: Fundamentals and Applications. *Small* **2020**, *16* (29), 2000171. https://doi.org/10.1002/smll.202000171.

31. Plouffe, B. D.; Murthy, S. K.; Lewis, L. H. Fundamentals and Application of Magnetic Particles in Cell Isolation and Enrichment: *A Review*. *Reports on Progress in Physics* **2015**, *78* (1), 016601. https://doi.org/10.1088/0034-4885/78/1/016601.

32. Durmus, N. G.; Tekin, H. C.; Guven, S.; Sridhar, K.; Arslan Yildiz, A.; Calibasi, G.; Ghiran, I.; Davis, R. W.; Steinmetz, L. M.; Demirci, U. Magnetic Levitation of Single Cells. *Proceedings of the National Academy of Sciences* **2015**, *112* (28), 3661–3668. https://doi.org/10.1073/pnas.1509250112.

33. Karakuzu, B.; Anil İnevi, M.; Tarim, E. A.; Sarigil, O.; Guzelgulgen, M.; Kecili, S.; Cesmeli, S.; Koc, S.; Baslar, M. S.; Oksel Karakus, C.; Ozcivici, E.; Tekin, H. C. Magnetic Levitation-Based Miniaturized Technologies for Advanced Diagnostics. *Emergent Mater* **2024**, *7* (1), 237–254. https://doi.org/10.1007/s42247-024-00762-6.

34. Yaman, S.; Tekin, H. C. Magnetic Susceptibility-Based Protein Detection Using Magnetic Levitation. *Anal Chem* **2020**, *92* (18), 12556–12563. https://doi.org/10.1021/acs.analchem.0c02479.

35. Subramaniam, A. B.; Gonidec, M.; Shapiro, N. D.; Kresse, K. M.; Whitesides, G. M. Metal-Amplified Density Assays, (MADAs), Including a Density-Linked Immunosorbent Assay (DeLISA). *Lab Chip* **2015**, *15* (4), 1009–1022. https://doi.org/10.1039/C4LC01161A.

36. Knowlton, S. M.; Sencan, I.; Aytar, Y.; Khoory, J.; Heeney, M. M.; Ghiran, I. C.; Tasoglu, S. Sickle Cell Detection Using a Smartphone. *Sci Rep* **2015**, *5* (1), 15022. https://doi.org/10.1038/srep15022.

37. Anil-Inevi, M.; Delikoyun, K.; Mese, G.; Tekin, H. C.; Ozcivici, E. Magnetic Levitation Assisted Biofabrication, Culture, and Manipulation of 3D Cellular

Structures Using a Ring Magnet Based Setup. *Biotechnol Bioeng* **2021**, *118* (12), 4771–4785. https://doi.org/10.1002/bit.27941.

38. Sarigil, O.; Anil-Inevi, M.; Yilmaz, E.; Ozcelik, O.; Mese, G.; Tekin, H. C.; Ozcivici, E. Magnetic Levitation-Based Adipose Tissue Engineering Using Horizontal Magnet Deployment. In 2020 Medical Technologies Congress (TIPTEKNO); *IEEE*, **2020**; pp 1–4. https://doi.org/10.1109/TIPTEKNO50054.2020.9299312.

39. Delikoyun, K.; Yaman, S.; Yilmaz, E.; Sarigil, O.; Anil-Inevi, M.; Telli, K.; Yalcin-Ozuysal, O.; Ozcivici, E.; Tekin, H. C. HologLev: A Hybrid Magnetic Levitation Platform Integrated with Lensless Holographic Microscopy for Density-Based Cell Analysis. *ACS Sens* **2021**, *6* (6), 2191–2201. https://doi.org/10.1021/acssensors.0c02587.

40. Delikoyun, K.; Demir, A. A.; Tekin, H. C. Label-Free Detection of Rare Cancer Cells Using Deep Learning and Magnetic Levitation Principle. In Label-free Biomedical Imaging and Sensing (LBIS). *SPIE*, **2021**; *10* (1), 1165509. https://doi.org/10.1117/12.2572908.

41. Aman, J.; Weijers, E. M.; van Nieuw Amerongen, G. P.; Malik, A. B.; van Hinsbergh, V. W. M. Using Cultured Endothelial Cells to Study Endothelial Barrier Dysfunction: Challenges and Opportunities. *American Journal of Physiology-Lung Cellular and Molecular Physiology* **2016**, *311* (2), 453–466. https://doi.org/10.1152/ajplung.00393.2015.

42. Huang, Z.; Liu, Z.; Wang, K.; Ye, Z.; Xiong, Y.; Zhang, B.; Liao, J.; Zeng, L.; Zeng, H.; Liu, G.; Zhan, H.; Yang, Z. Reduced Number and Activity of Circulating Endothelial Progenitor Cells in Acute Aortic Dissection and Its Relationship With IL-6 and IL-17. *Front Cardiovasc Med* **2021**, *8* (1), 628462. https://doi.org/10.3389/fcvm.2021.628462.

43. Chen, K.-C.; Lee, T.-P.; Pan, Y.-C.; Chiang, C.-L.; Chen, C.-L.; Yang, Y.-H.; Chiang, B.-L.; Lee, H.; Wo, A. M. Detection of Circulating Endothelial Cells via a Microfluidic Disk. *Clin Chem* **2011**, *57* (4), 586–592. https://doi.org/10.1373/clinchem.2010.157404.

44. Liu, F.; KC, P.; Zhang, G.; Zhe, J. Microfluidic Magnetic Bead Assay for Cell Detection. *Anal Chem* **2016**, *88* (1), 711–717. https://doi.org/10.1021/acs.analchem.5b02716.

45. Chen, S.; Sun, Y.; Neoh, K. H.; Chen, A.; Li, W.; Yang, X.; Han, R. P. S. Microfluidic Assay of Circulating Endothelial Cells in Coronary Artery Disease Patients with Angina Pectoris. *PLoS One* **2017**, *12* (7), e0181249. https://doi.org/10.1371/journal.pone.0181249.

46. Magbanua, M. J. M.; Pugia, M.; Lee, J. S.; Jabon, M.; Wang, V.; Gubens, M.; Marfurt, K.; Pence, J.; Sidhu, H.; Uzgiris, A.; Rugo, H. S.; Park, J. W. A Novel Strategy for Detection and Enumeration of Circulating Rare Cell Populations in Metastatic Cancer Patients Using Automated Microfluidic Filtration and Multiplex Immunoassay. *PLoS One* **2015**, *10* (10), e0141166. https://doi.org/10.1371/journal.pone.0141166.

47. Miranda, I.; Souza, A.; Sousa, P.; Ribeiro, J.; Castanheira, E. M. S.; Lima, R.; Minas, G. Properties and Applications of PDMS for Biomedical Engineering: A Review. *J Funct Biomater* **2021**, *13* (1), 2. https://doi.org/10.3390/jfb13010002.

48. Sales, F. C. P.; Ariati, R. M.; Noronha, V. T.; Ribeiro, J. E. Mechanical Characterization of PDMS with Different Mixing Ratios. *Procedia Structural Integrity* **2022**, *37*, 383–388. https://doi.org/10.1016/j.prostr.2022.01.099.

49. Kim, S.; Kim, J.; Joung, Y.-H.; Choi, J.; Koo, C. Bonding Strength of a Glass Microfluidic Device Fabricated by Femtosecond Laser Micromachining and Direct Welding. *Micromachines (Basel)* **2018**, *9* (12), 639. https://doi.org/10.3390/mi9120639.

50. Medina-Leyte, D. J.; Domínguez-Pérez, M.; Mercado, I.; Villarreal-Molina, M. T.; Jacobo-Albavera, L. Use of Human Umbilical Vein Endothelial Cells (HUVEC) as a Model to Study Cardiovascular Disease: A Review. *Applied Sciences* **2020**, *10* (3), 938. https://doi.org/10.3390/app10030938.

51. Breuls, R. G. M.; Mol, A.; Petterson, R.; Oomens, C. W. J.; Baaijens, F. P. T.; Bouten, C. V. C. Monitoring Local Cell Viability in Engineered Tissues: A Fast, Quantitative, and Nondestructive Approach. *Tissue Eng* **2003**, *9* (2), 269–281. https://doi.org/10.1089/107632703764664738.

52. Bortner, C. D.; Cidlowski, J. A. Apoptotic Volume Decrease and the Incredible Shrinking Cell. *Cell Death Differ* **2002**, *9* (12), 1307–1310. https://doi.org/10.1038/sj.cdd.4401126.

53. Voronin, D. V.; Kozlova, A. A.; Verkhovskii, R. A.; Ermakov, A. V.; Makarkin, M. A.; Inozemtseva, O. A.; Bratashov, D. N. Detection of Rare Objects by Flow

Cytometry: Imaging, Cell Sorting, and Deep Learning Approaches. *Int J Mol Sci* **2020**, *21* (7), 2323. https://doi.org/10.3390/ijms21072323.

54. Islam, M.; Brink, H.; Blanche, S.; DiPrete, C.; Bongiorno, T.; Stone, N.; Liu, A.; Philip, A.; Wang, G.; Lam, W.; Alexeev, A.; Waller, E. K.; Sulchek, T. Microfluidic Sorting of Cells by Viability Based on Differences in Cell Stiffness. *Sci Rep* **2017**, *7* (1), 1997. https://doi.org/10.1038/s41598-017-01807-z.

55. Elliot K. Chin; Colin A. Grant; Mehmet Giray Ogut; Bocheng Cai; Naside Gozde Durmus. CelLEVITAS: Label-Free Rapid Sorting And Enrichment Of Live Cells Via Magnetic Levitation. *bioRxiv* **2020**, (1), 223917. https://doi.org/10.1101/2020.07.27.223917.

56. Saraiva, D. P.; Matias, A. T.; Braga, S.; Jacinto, A.; Cabral, M. G. Establishment of a 3D Co-Culture With MDA-MB-231 Breast Cancer Cell Line and Patient-Derived Immune Cells for Application in the Development of Immunotherapies. *Front Oncol* **2020**, *10* (1). https://doi.org/10.3389/fonc.2020.01543.